カソードワークショップ報告

第48回ERL検討会

2010年11月9日

山本将博

1st P3 workshop @ BNL

期間：10月12日～14日の3日間
参加者：総勢40人程度

Topics

・カソードの加速器利用の現状
・カソードの作成手法
・カソードの解析の最新情報
・光電子のスペクトル解析
・カソード解析のための諸施設の利用
・光電子放出の理論
・将来のカソード開発案
・カソード開発、評価の協力関係について

USA groups

BNL, ANL, Cornell, SLAC, JLAB, UCLA, LBNL, PNNL, IBM, U. Maryland

Europe groups

Daresbury, PSI, HZB

Asia groups

KEK/Nagoya （山本・桑原の2名）

各所の電子銃・フォトカソード

RF電子銃
常伝導型：BNL(CsK2Sb,diamond),　ANL(Cs2Te,CsK2Sb),
SLAC(Cu),　LBNL(CsK2Sb),　UCLA(Cu,Nb,MgF2)
U. Maryland (dispenser W cathode)
超伝導型：HZB(Nb,Pb,CsK2Sb..)

DC電子銃
パルス：PSI (Cu, Mg, Ti, SUS, Bronze, Y, Al, Mo, Nb, FEA)
CW：　Cornell(GaAs, AlGaAs) ,　JLAB(2-photon GaAs),
SLAC(GaAs (Li)),　Daresbury(GaAs),
KEK/Nagoya (Superlattice)

RF電子銃関連のグループからの報告が7割程度。
発表スライドは下記よりダウンロード可能。
https://indico.bnl.gov/conferenceDisplay.py?confId=290

NGLS: Motivation for LBNL Photocathode Research

H. Padmore (LBNL)

RF photo-injector for high rep rate X-FEL

- repetition rates up to ~ 1 MHz
- charge per bunch from tens of pC to ~ 1 nC
- < 10^{-7} (low charge) to 10^{-6} m normalized emittance
- beam energy at the gun exit > than 500 keV
- E field at cathode > 10 MV/m
- bunch length from tens of fs to tens of ps

- 10^{-9} - 10^{-11} Torr operation vacuum pressure allows for high QE photo-cathodes!

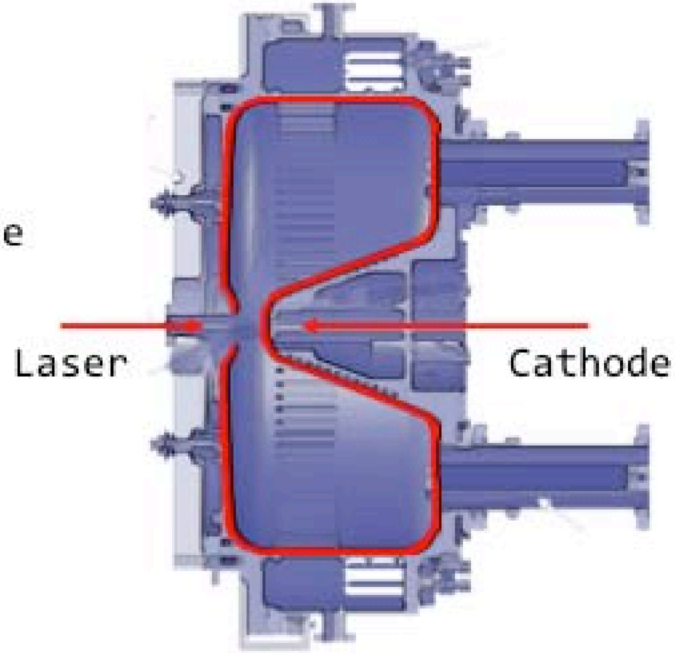

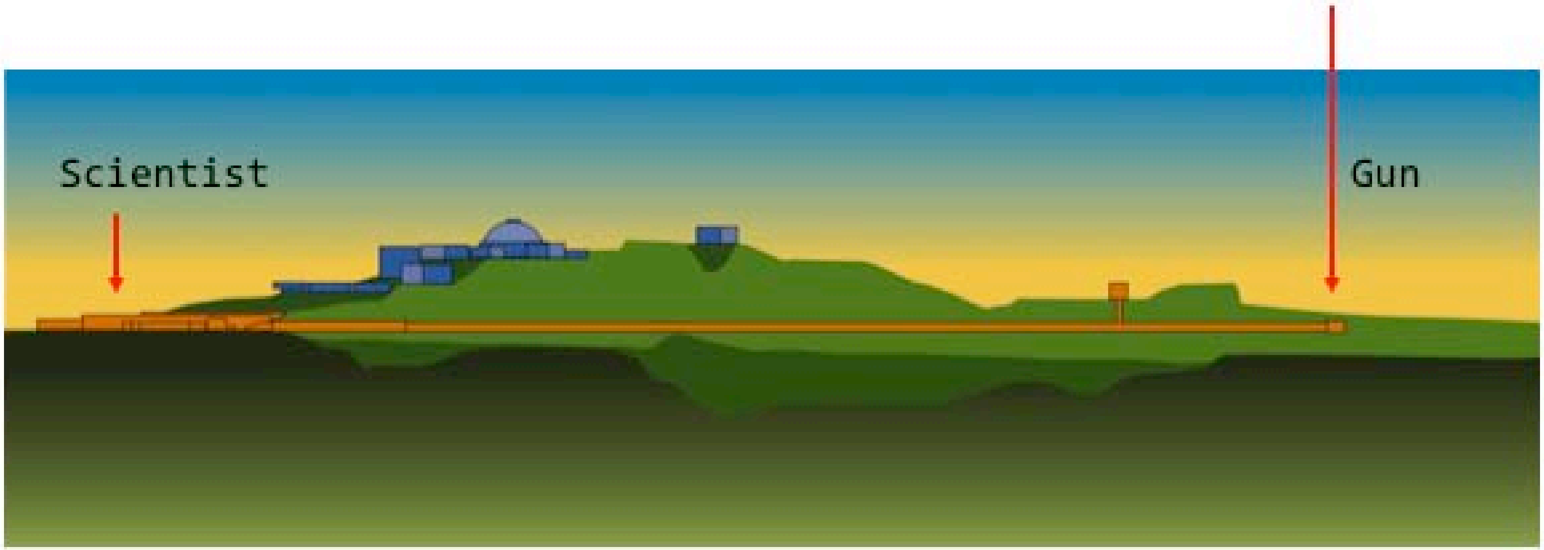

LBNL Photocathodes

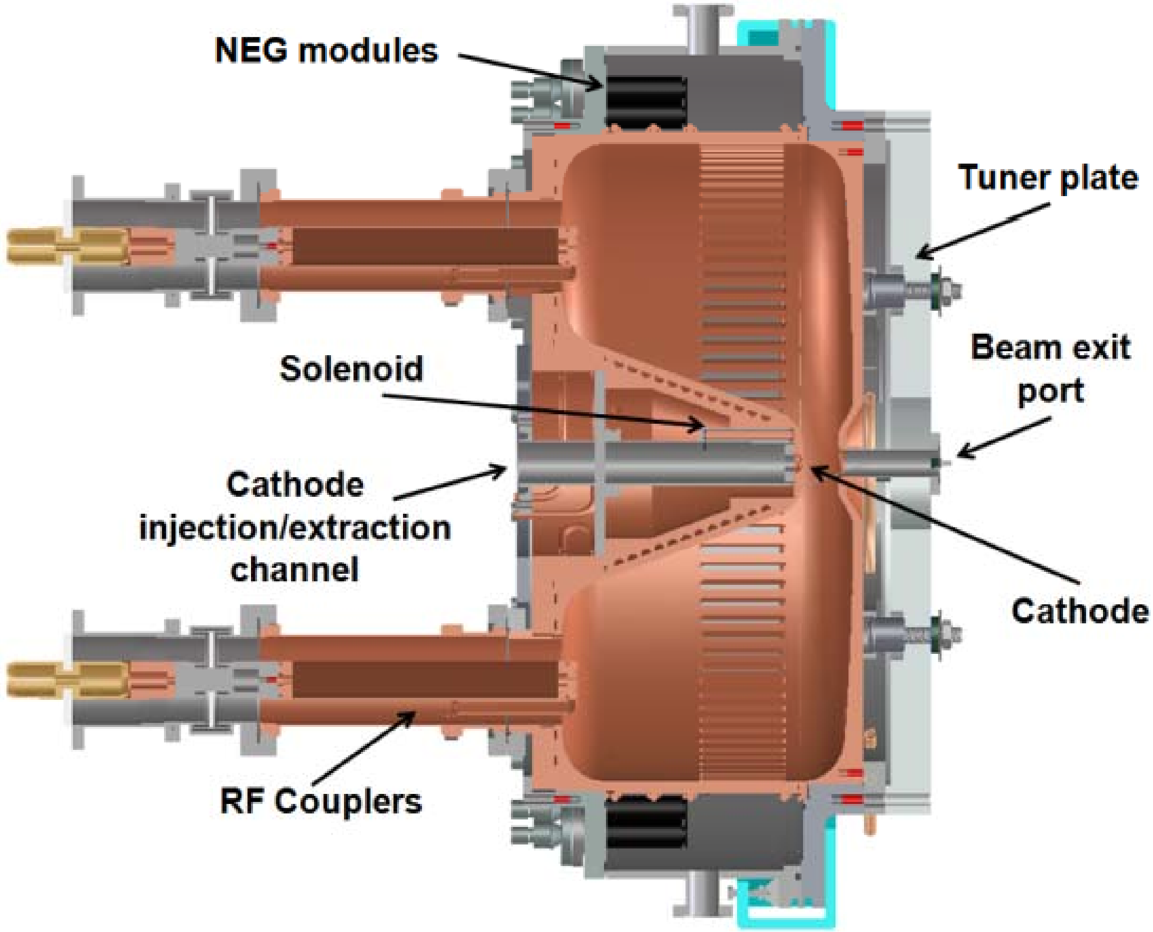

Frequency	187 MHz
Operation mode	CW
Gap voltage	750 kV
Field at the cathode	19.47 MV/m
Q_0	30887
Shunt impedance	6.5 MΩ
RF Power	87.5 kW
Stored energy	2.3 J
Peak surface field	24.1 MV/m
Peak wall power density	25.0 W/cm^2
Accelerating gap	4 cm
Diameter	69.4 cm
Total length	35.0 cm

INFN – FLASH cathode load lock / transfer system

Learning from 60 Year History of Bialkali PMTs

H. Padmore (LBNL)

Hamamatsu
PMT leader
4k employees
$200 M PMT sales

Super-Kamiokande
Neutrino Detector
11,200 20”
K_2CsSb PMTs

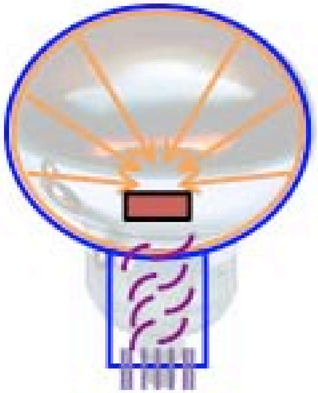

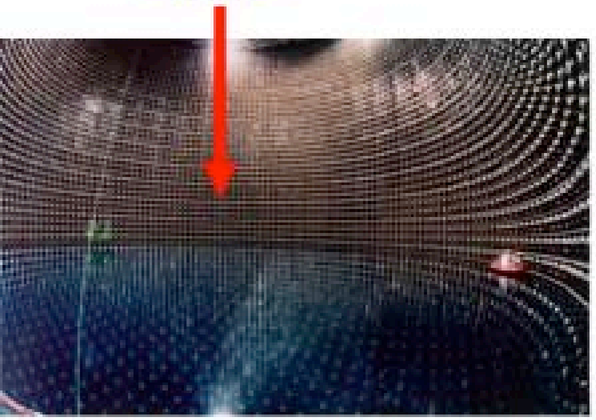

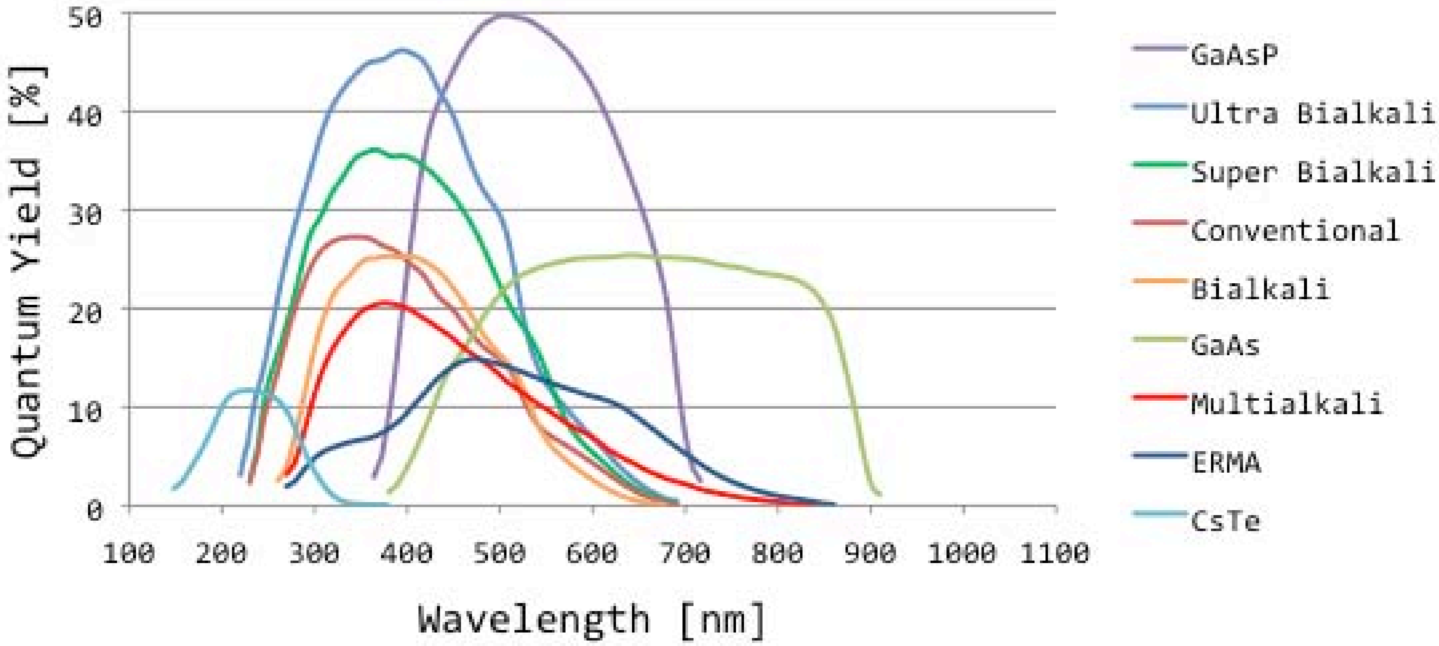

Source: Motohiro Suyama PoS(PD07)018 [Hamamatsu]

[MIRZOYAN R, 2007, NUCL INSTRUM METH PHYS RES A, V572, P449]
ENHANCED QUANTUM EFFICIENCY BIALKALI PHOTO MULTIPLIER TUBES

Classical bialkali PMTs peak QE ~ 25-27% (+40 years ago)
New bialkali PMTs with peak QE ~ 30-35%

Factors that enhance QE of PMTs:
1) pure materials (e.g. > 99.9999%) provides less e- scattering
   i.e. e⁻ excited deep in bulk can contribute to emitted current
2) thickness - determines the peak position of max QE
3) composition - provides a wide and high spectral response..

Low Temperature Effusion Cells for Sb, Cs and K

H. Padmore (LBNL)

Dr. Eberl MBE-Komponenten GmbH

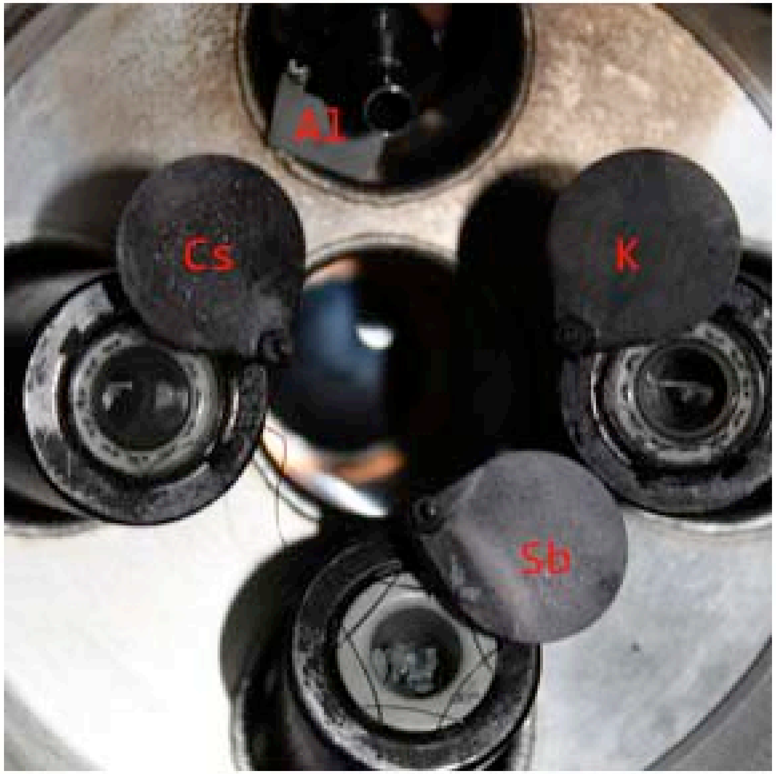

Alvatec Alkali Sources

After 24 h @ 200 °C there is still indium at the entrance of the source

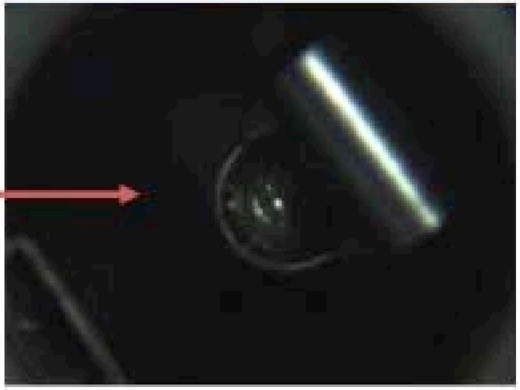

Increasing temperature to 300 °C and the indium appears to disappear in 10-15 min

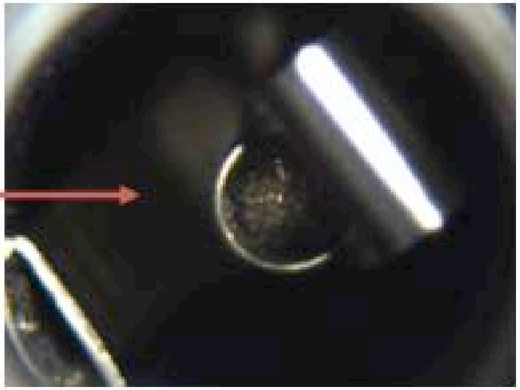

the last thing a new cathode ever sees…

Much More Simple Recipe Yields Same Result

H. Padmore (LBNL)

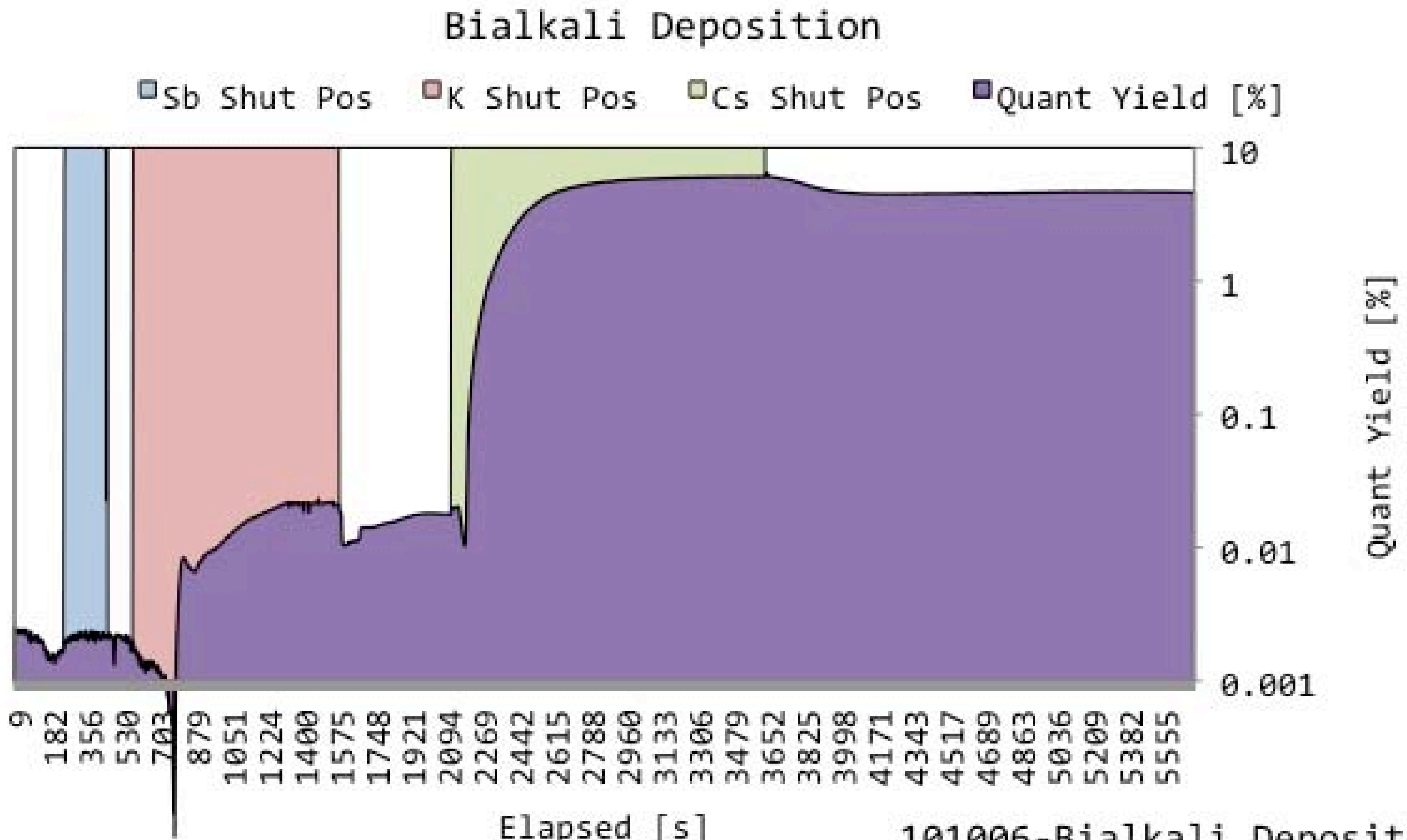

101006-Bialkali Deposition.XLSX

Initially cathode cleansed at 600 °C

200 Å deposition of Sb at 190 °C

Deposition of K at 140 °C

Deposition of Cs at 120 °C

Max QE reached 6%, stabalized after cooling to r.t. at 4.5%

Characterization of K_2CsSb using X-Ray Techniques

H. Padmore (LBNL)

- mixture of Mo substrate (continuous) and antimonide diffraction (discontinuous rings)
- dots in rings are individual single grain reflections
- indicates grainy thin film (see AFM)
- radial integration with Mo subtracted
- double peaks indicate 2 phase material

Aluminum Mo Alkali

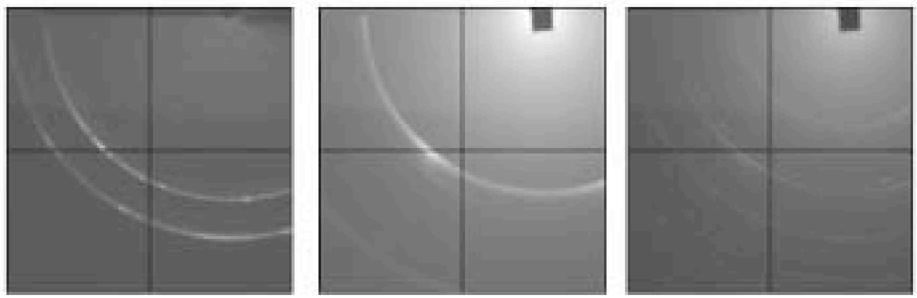

XRD - 0.7° grazing incidence

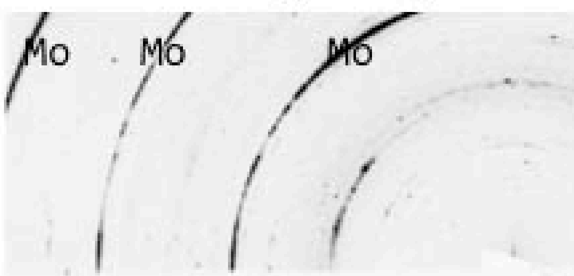

On large K,Cs-rich particle

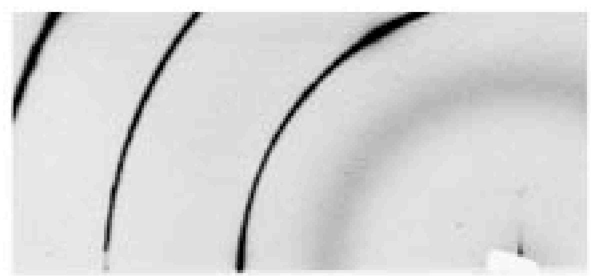

Off large particle

X-ray photoelectron spectroscopy (XPS)

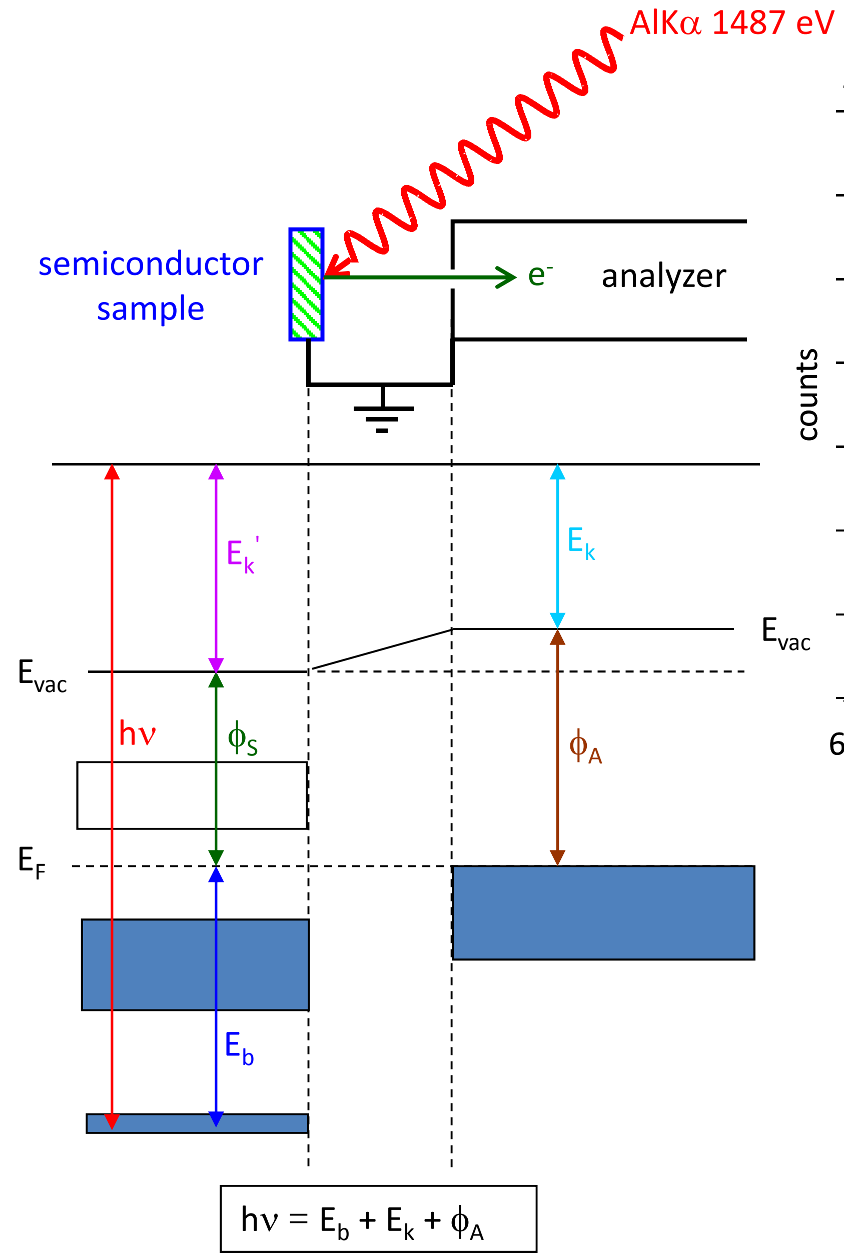

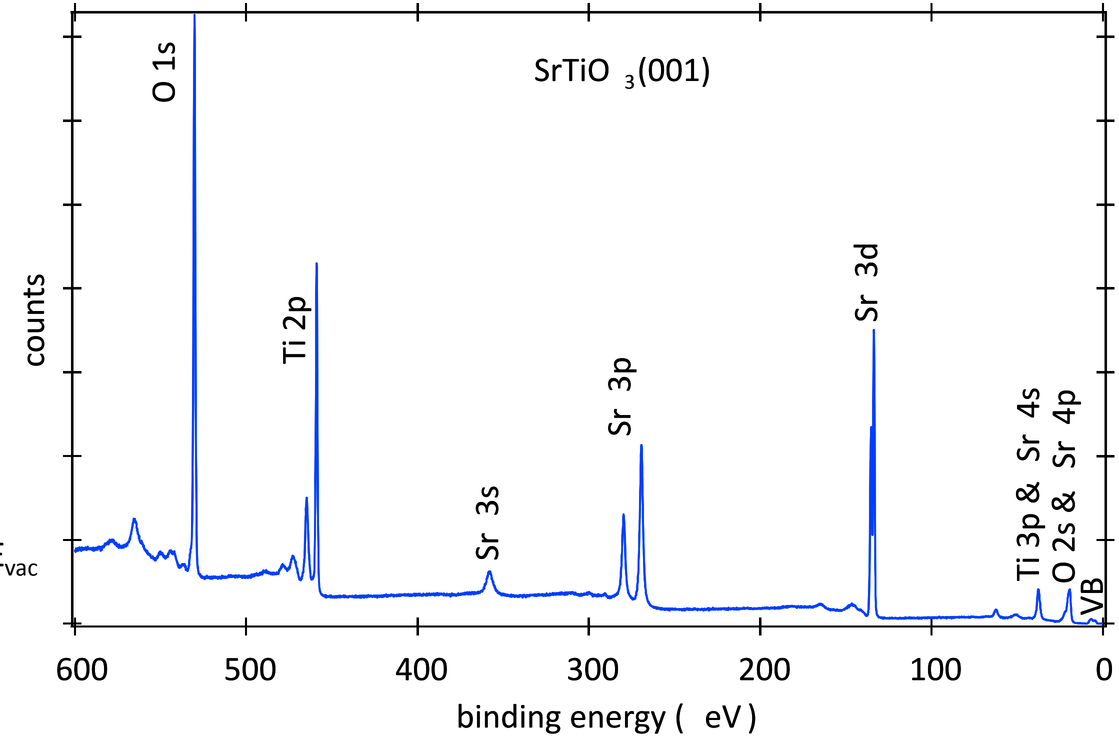

Scott A. Chambers (PNNL)

UV photoelectron spectroscopy (UPS)

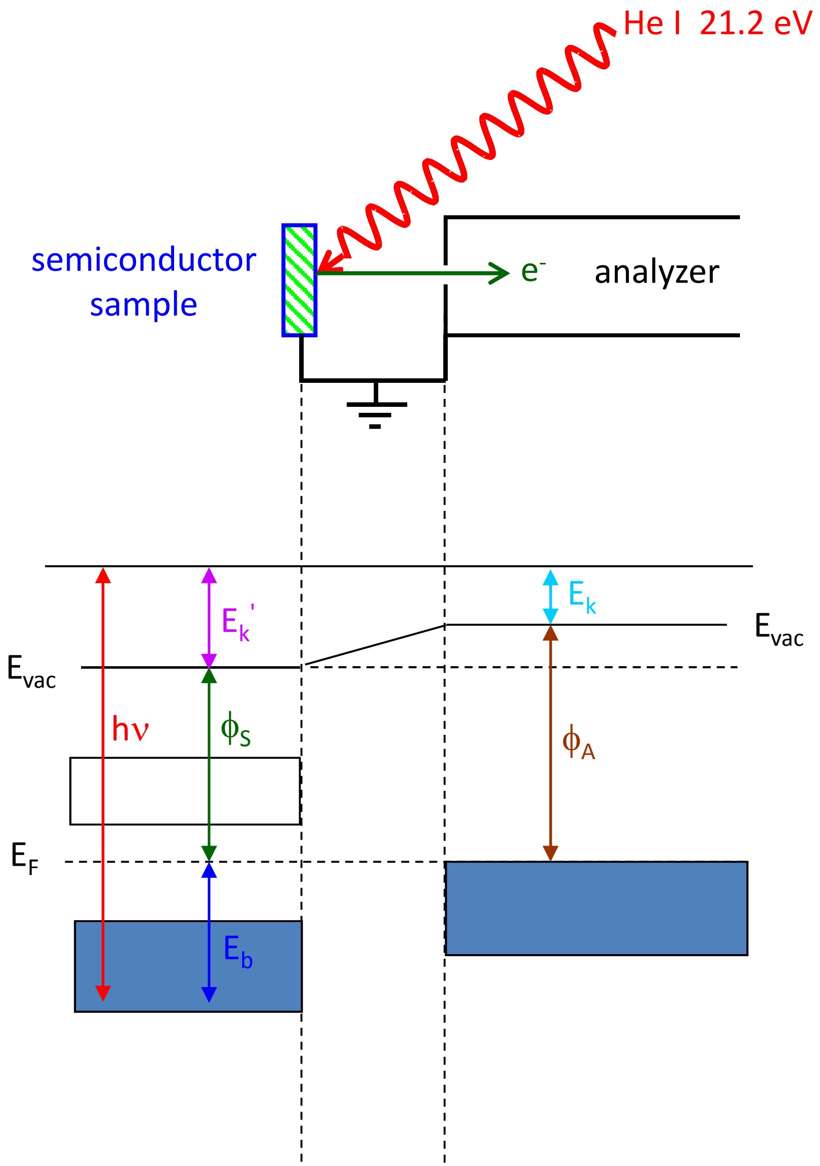

$h\nu = E_b + E_k + \phi_A$

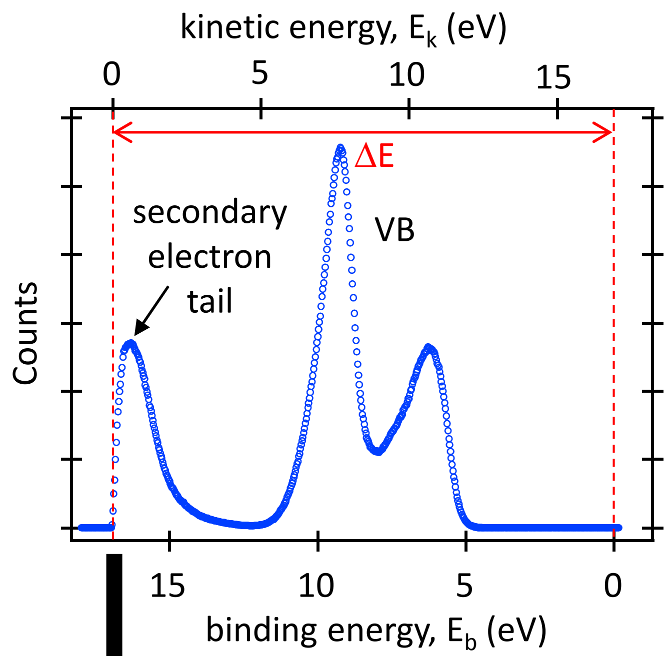

$\Delta E = h\nu - \phi_S$

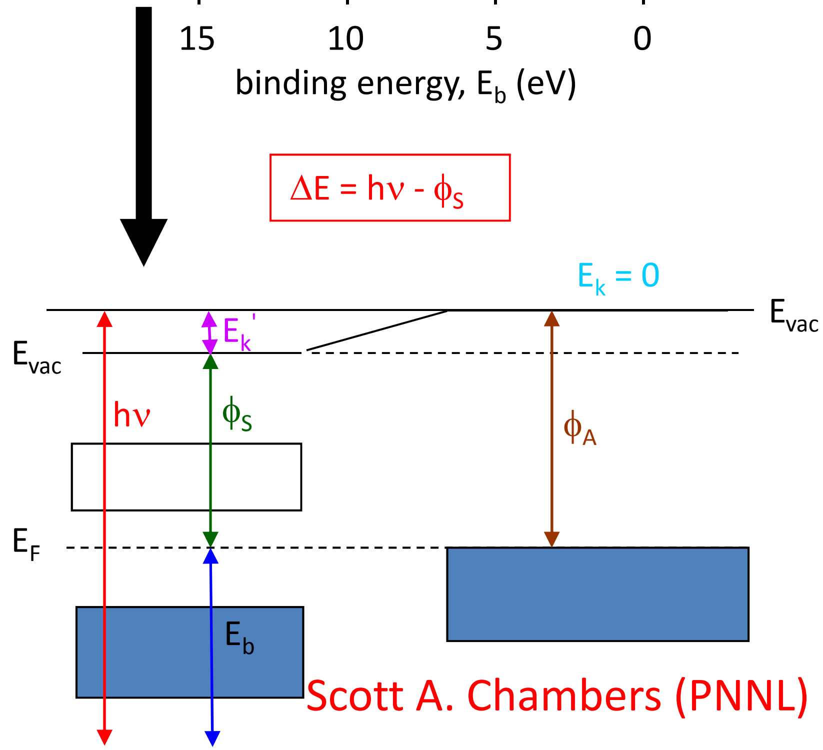

Scott A. Chambers (PNNL)

High-energy resolution XPS/UPS spectrometer

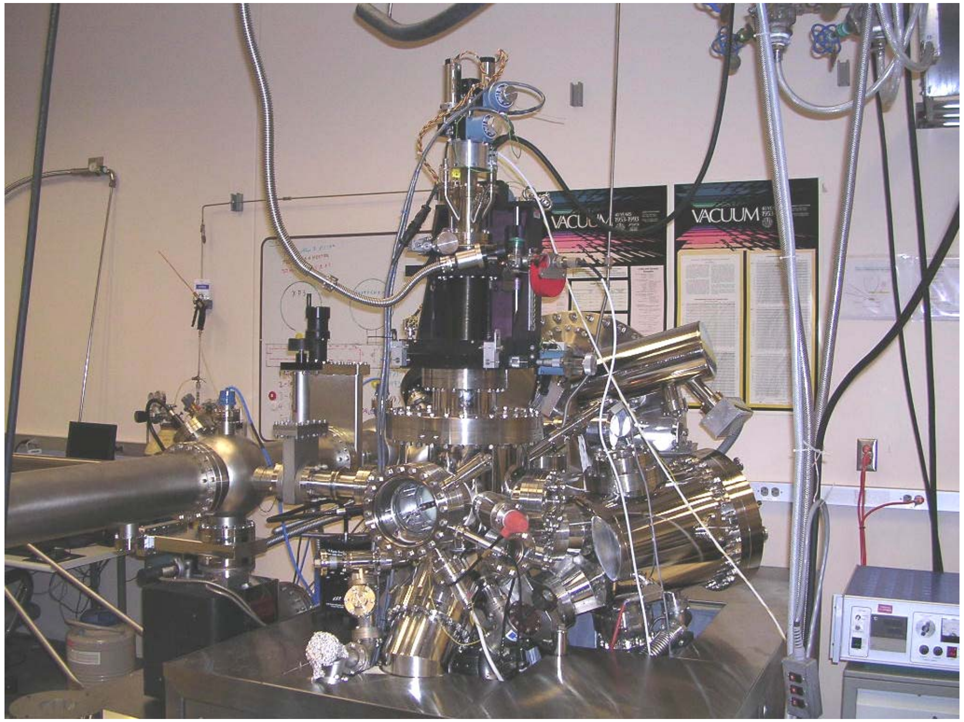

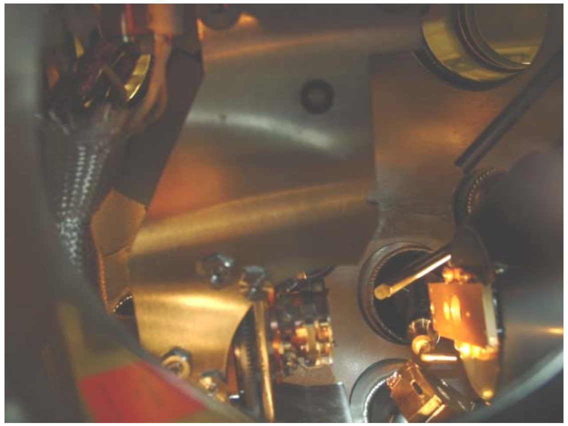

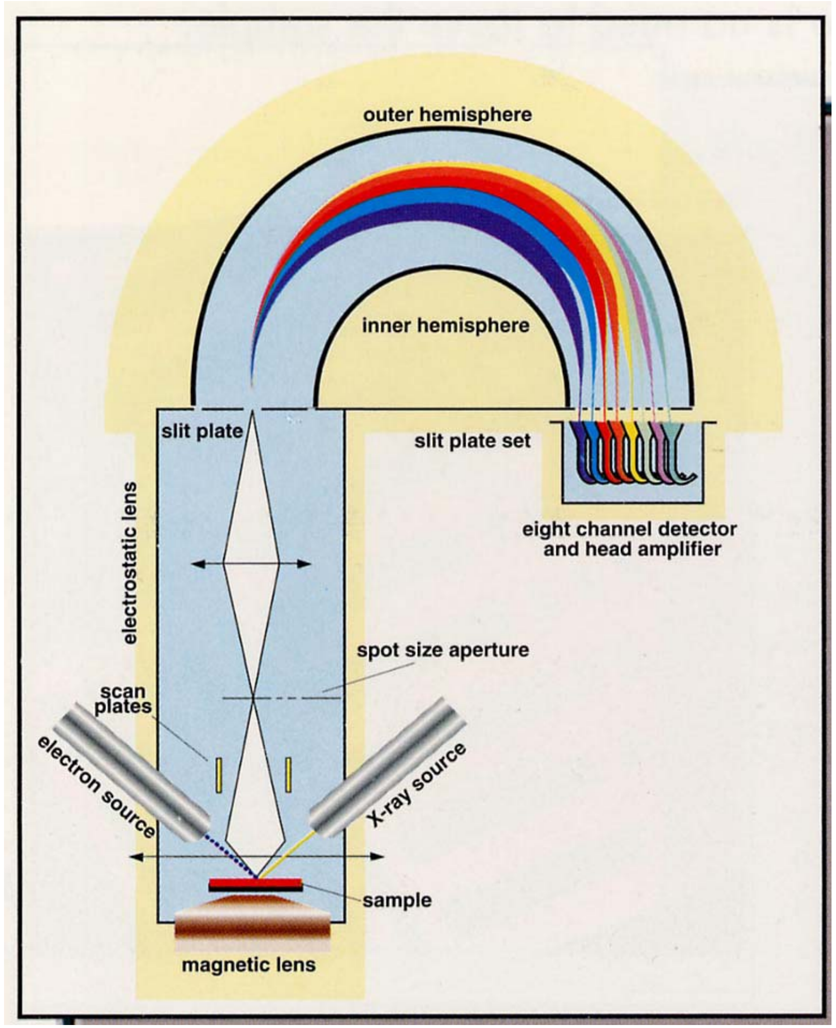

Scott A. Chambers (PNNL)

n-Si(001)-(2x1)
XPS VB & GGA

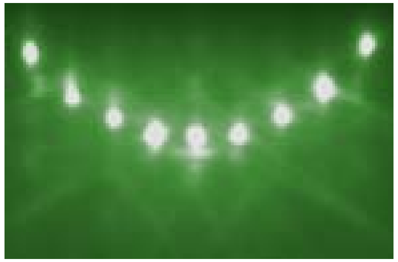

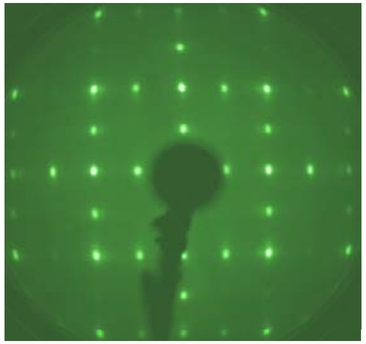

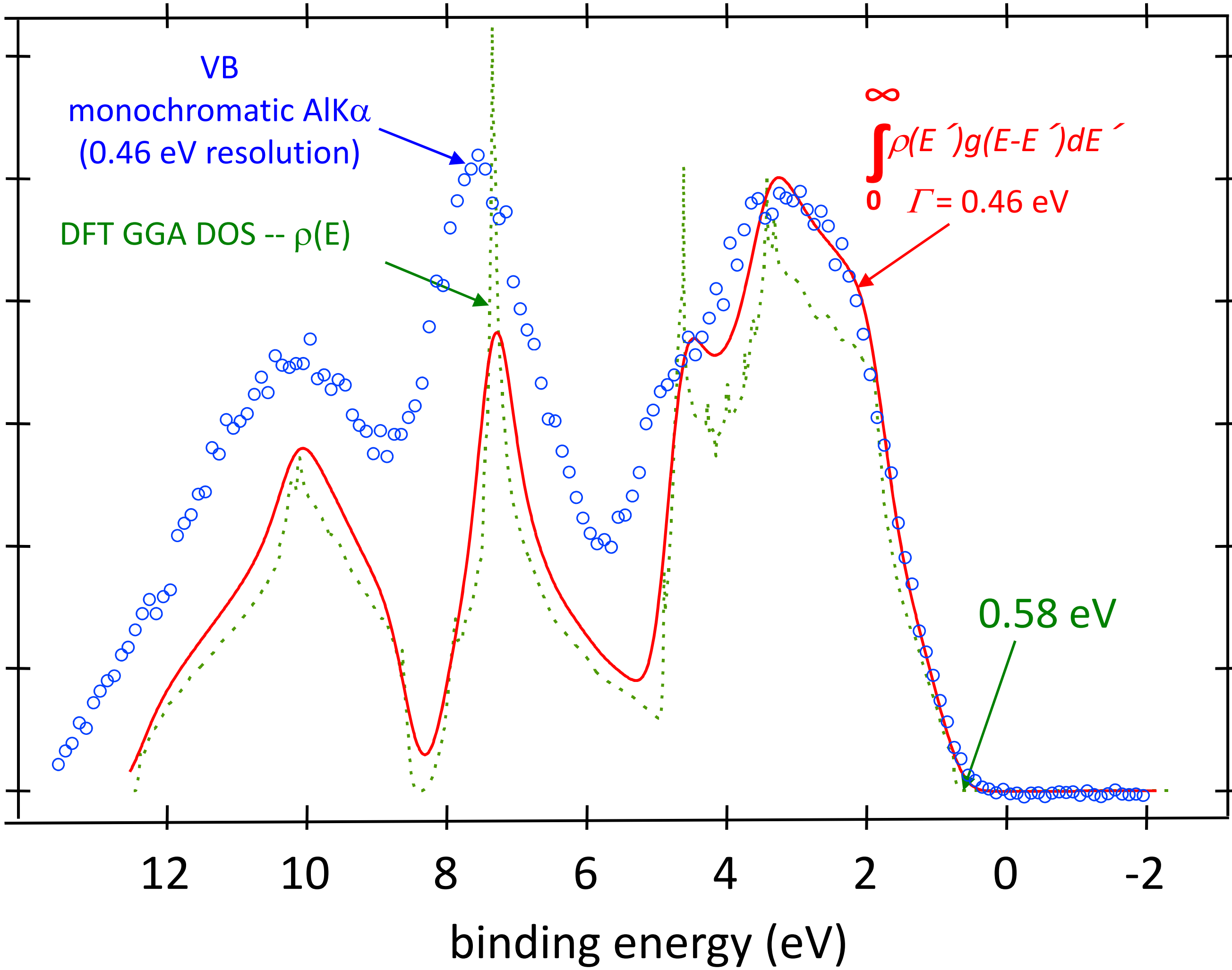

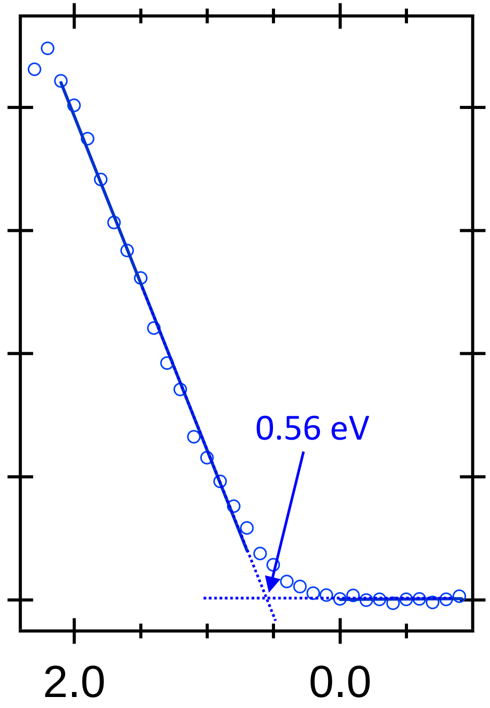

Scott A. Chambers (PNNL)

Diamond Science at BNL

J. Smedley (BNL)

Imaging

SEM	Scanning Electron Microscopy	Surface morphology
LEEM	Low Energy Electron Microscopy	Imaging of hydrogenated surface, spatially localized LEED, work function mapping
AFM	Atomic Force Microscopy	Surface morphology

Diffraction

XRD	X-ray diffraction, time resolved	Characterization of metal contacts, including temperature of formation and crystalline texture
XRD	X-ray diffraction	Diamond crystal quality; evaluation of stress caused by laser shaping
Topography		Diamond crystal quality, localization and identification of defects
LEED	Low Energy Electron Diffraction	Surface crystal analysis, evaluation of hydrogenated surface

Spectroscopy

UPS/ARPES	Ultraviolet Photoemission Spectroscopy	Electron affinity, energy & angular distribution of emitted electrons, lifetime of NEA surface
TYS	Total Yield Spectroscopy	Evaluation of hydrogenated surface, lifetime
NEXAFS	Near Edge X-ray Absorption Fine Structure	Surface elemental analysis, characterization of surface bonding, carbon formation
XAFS	X-ray absorption fine structure	Titanium/diamond surface chemistry
EDS	Energy Dispersive X-ray Spectroscopy	Surface elemental analysis
FTIR	Fourier Transform Infrared Spectroscopy	Impurities in diamond
Photoluminescence & Raman Spectroscopy		Impurity analysis, identification of carbon chemistry, mapping

Carrier Transport and Emission

Electron Generated	Carrier Transport vs Field, Emission, Gain, Thermal Emittance
Photo-electron Generated	Gain, Timing
Soft X-ray, Monochromatic	Charge collection distance, Charge trapping/detrapping effects
Hard X-ray, Monochromatic	Measurement of mean ionization energy (gain)
High Flux White beam	Current Limits, Contact requirements, Heat management
Micro-beam Mapping	Localization of electrically active sites

EQUATIONS OF ELECTRON EMISSION

K. L. Jensen (NRL)

$$J(F,T) = \frac{1}{2\pi\hbar}\int_0^\infty D(E)f(E)dE$$

THERMAL
Low Field, High Temperature
Richardson-Laue-Dushman Eq.

$$D(E) = \Theta\left[E-(\mu+\Phi)\right]$$

$$f(E) = \frac{mk_B T}{\pi\hbar^2}\exp\left[(\mu-E)/k_B T\right]$$

$$J_{RLD}(T) = \left(\frac{mk_B^2}{2\pi^2\hbar^3}\right)T^2\exp\left[-\Phi/k_B T\right]$$

$T = 1273$ K
$\Phi = 2.1$ eV

$J_{RLD} \approx 1$ A/cm^2

Thermionic cathodes run at lower T levels than possible to preserve lifetime

FIELD
High Field, Low Temperature
Fowler Nordheim Eq.

$$D(E) \approx \exp\left[-(B/F)-C(\mu-E)\right]$$

$$f(E) = \frac{m}{\pi\hbar^2}(\mu-E)\Theta(\mu-E)$$

$$J_{FN}(F) = \frac{F^2}{16\pi^2\hbar\Phi}\exp(-B/F)$$

$$B = \frac{4}{3\hbar}\sqrt{2m\Phi^3};\quad C = \frac{2}{\hbar F}\sqrt{2m\Phi}$$

$F = 7$ GV/m
$\Phi = 4.5$ eV

$J_{RLD} \approx 1.5\text{x}10^5$ A/cm^2

Field emission occurs over (5 nm)^2 emission areas

PHOTO
Low Field & Temp, Photon
Fowler-Dubridge Relation

$$D(E) = \Theta\left[E+\hbar\omega-(\mu+\Phi)\right]$$

$$f(E) = \frac{m}{\pi\hbar^2}(\mu-E)\Theta(\mu-E)$$

$$J_{FD}(\hbar\omega) = \frac{m}{4\pi^2\hbar^3}(\hbar\omega-\Phi)^2$$

$\hbar\omega = 4.66$ eV

$\Phi = 4.5$ eV, $\mu = 7$ eV

$$QE_{FD} \approx \frac{J_{over}}{J_{all}} = \frac{(\hbar\omega-\Phi)^2}{\mu^2}$$

$$= 0.1\%$$

Losses due to scattering lowers estimate

More? See K.L. Jensen. J. Appl. Phys. 102, 024911 (2007).

EMITTANCE EVALUATION BY MOMENTS APPROACH

Transverse Moments Evaluation for Metals & Semiconductors

K. L. Jensen (NRL)

Moments Approach can be used to calculate the weighted averages used in calculation of emittance

$$M_n = (2\pi)^{-3}\left(\frac{2m}{\hbar^2}\right)^{3/2}\int_0^\infty E^{1/2}\,dE\int_0^{\pi/2}\sin\theta\,d\theta\left\{\frac{2m}{\hbar^2}(E+\hbar\omega)\sin^2\theta\right\}^{n/2} D\left\{(E+\hbar\omega)\cos^2\theta\right\} f_\lambda\left[\cos\theta, p(\hbar\omega)\right]\begin{cases} f_{FD}(E)\left(1-f_{FD}(E+\hbar\omega)\right) \\ \Theta\left(\hbar\omega+E-E_g\right)\end{cases}$$

Important: Cons. of **k** across surface for k_x & k_y of wave function demands appending photon energy to E in moment term
Dowell, Schmerge, PRSTAB 12, 074201 (2009).

This is transverse momentum (sin would be cos for J calc)

This is transmission probability for surface barrier

This is scattering loss factor for bulk transport

This is initial & final state occupation factor

$$\varepsilon_{n,rms} = \frac{\hbar}{mc}\sqrt{\langle x^2\rangle\langle k_x^2\rangle - \langle xk_x\rangle^2}$$

<...> in ε are weighted over f(x,k) of emitted electrons, and therefore already in language of Moments

$$\langle O(x,k_x)\rangle \equiv \int d\mathbf{r}\,d\mathbf{k}\,O(x,k_x)\,f(\mathbf{r},\mathbf{k})$$

THERMAL EMISSION

No photons	$\hbar\omega = 0$
Uniform emission	$2\langle x^2\rangle = \langle \rho^2\rangle = \rho_c^2$
Richardson Approx.	$D(k) = \Theta(E(k)-\mu-\phi)$
No Scattering	$f_\lambda(x,p) = 1$
Maxwell-Boltzmann f(x,k)	$D(k)f(k) \propto \exp\{-(E(k)-\mu)/k_BT\}$
No "Final state" issues	$1-f_{FD}(E) \Rightarrow 1$

$$\varepsilon_{n,rms}(thermal) = \frac{\hbar}{mc}\sqrt{\langle x^2\rangle\langle k_x^2\rangle} = \frac{\hbar}{mc}\left(\frac{\rho_c}{2}\right)\left(\frac{M_2}{2M_0}\right)^{1/2} = \frac{\rho_c}{2}\left(\frac{k_BT}{mc^2}\right)^{1/2}$$

PHOTO-EMISSION

Photons	$\hbar\omega > 0$
Uniform emission	$2\langle x^2\rangle = \langle \rho^2\rangle = \rho_c^2$
JWKB Approx.	$D(k) = D_{JWKB}(E,F)$
Scattering	$f_\lambda(x,p) = x/(x+p(E))$
Schottky Lowering	$\phi = \Phi - \sqrt{q^2F/4\pi\varepsilon_0}$ leading order (metal)

$$\varepsilon_{n,rms}(photo) = \frac{\hbar}{mc}\left(\frac{\rho_c}{2}\right)\left(\frac{M_2}{2M_0}\right)^{1/2} \approx \frac{\rho_c}{2}\left[\frac{(\hbar\omega-\phi)}{3mc^2}\right]^{1/2}$$

Metals p large & $f_\lambda \approx \cos\theta/p$: therefore, emittance indep. of p.

Semiconductors larger ε due to p small, but D also has impact

COPPER: SIMULATION

- Start with 4000 electrons
- Laser penetration depth = 12 nm, incident from bottom of frame;
- λ = 266 nm, **Φ = 4.5 eV,** F = 50 MV/m, T = 300 K
- Time Step = 0.2 fs / frame, 100 frames Sim Region 20 nm x 20 nm
- When electron energy drops below barrier height $E < \mu + \Phi - (4QF)^{1/2}$, electron is removed from simulation visualization

- Left: "Fatal Scattering" Approx

K. L. Jensen (NRL)

- Right:
  - Acoustic changes electron direction
  - e-e bleeds away energy by creating 2nd electron & sharing KE, final direction is along one of 6 axes wrt incident direction
- Red electrons travel towards surface (down) Blue electrons travel away from surface (up)

caveat: pseudo-Monte Carlo

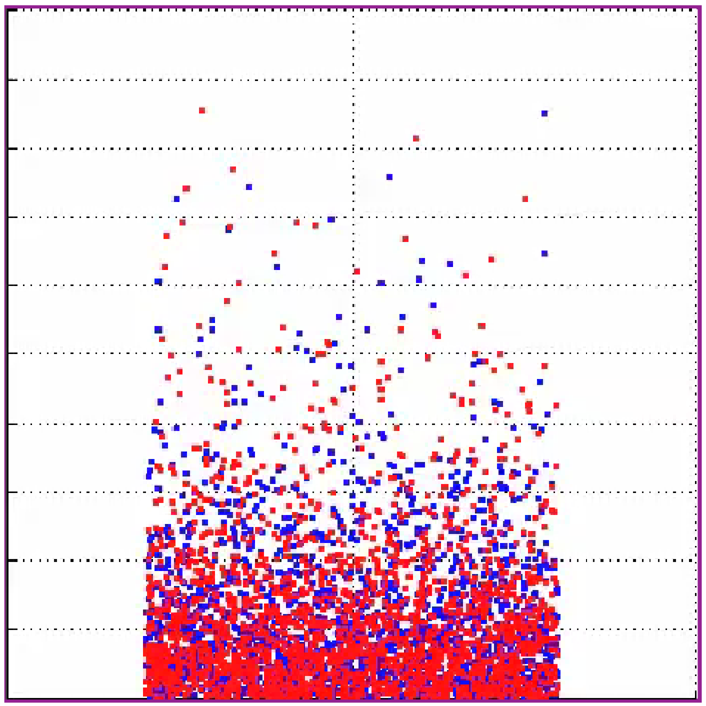

Approx: Scattering is fatal

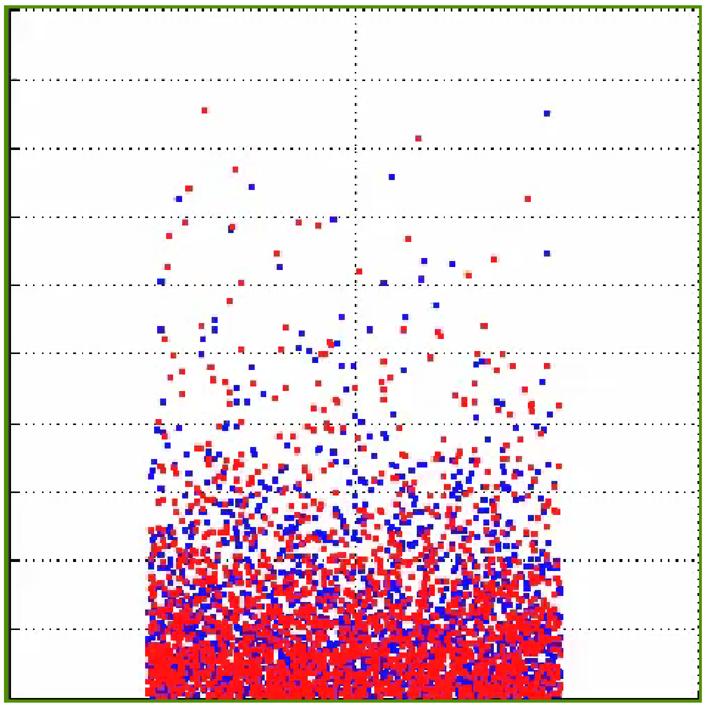

Approx: Scattering redirects & shares energy

If initial velocities of two colliding e- are p_z & q_z, where +z is direction of incident electron p_z and q_z is velocity of any allowed second electron, then:

- $p' = (p_z q_z)^{1/2}$
  $q' = (p_z^2 + q_z^2 - p_z q_z)^{1/2}$
  and $\theta = 0$ (π reverses role)
  with 33% Probability
- $p' = p_z$
  $q' = q_z$
  and $\theta = \pi/2$
  with 67% Probability

Current Status at HZB – sc-cavity (HoBiCaT) 2

At the moment the laser (I. Will, MBI) and electron-beam diagnostics are arranged

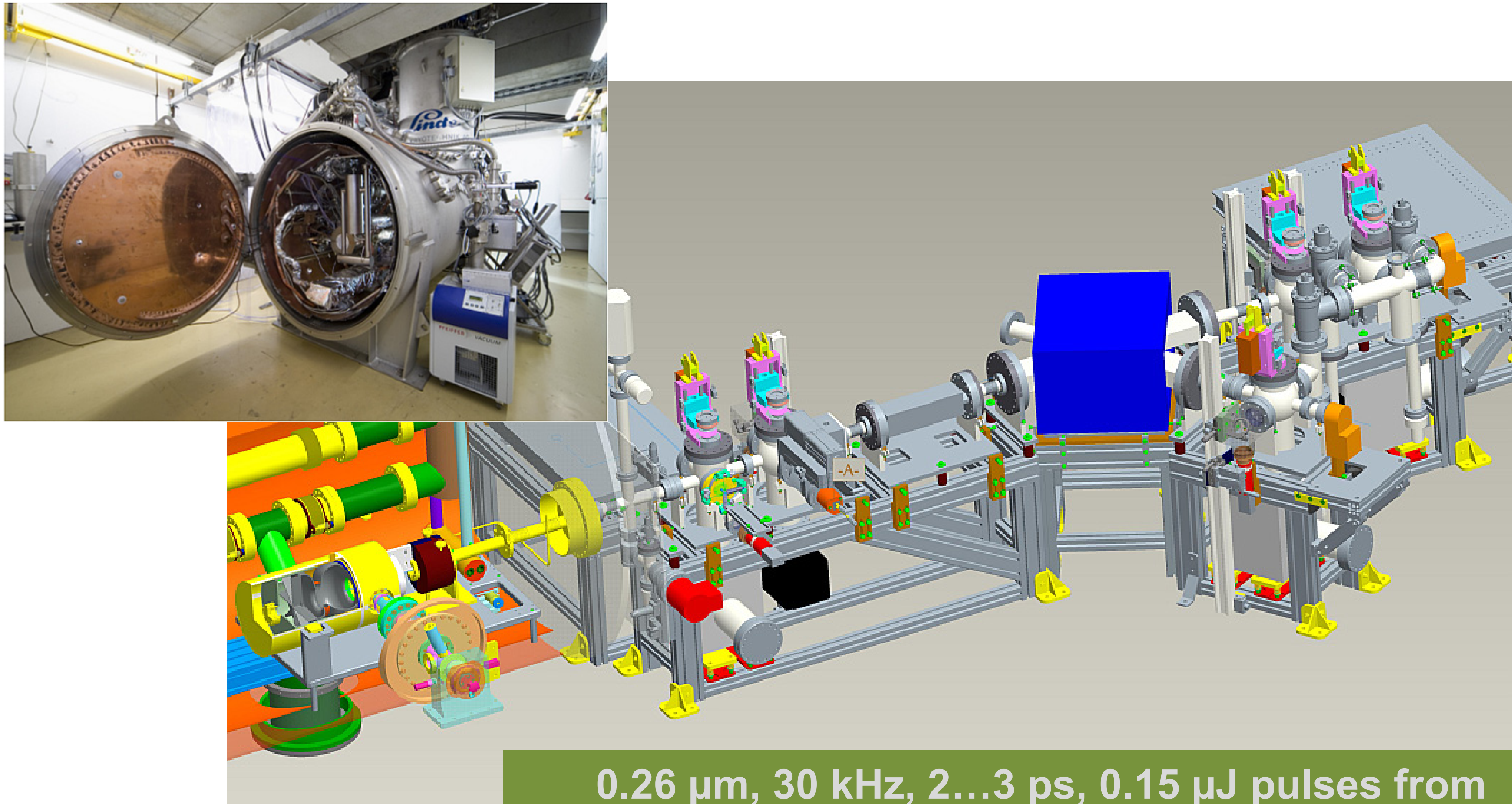

0.26 µm, 30 kHz, 2…3 ps, 0.15 µJ pulses from Yb:YAG oscillator + regen. amp. + 4th harm conv.

Design of UHV - chambers for CsK_2Sb - preparation:

p= 10^{-11} mbar range

plug-system from FZ-Dresden for possible sample exchange

still in search of a nice and suitable methode to heat the substrate (laser, boralectric…) and measure its temperature (pyrometer, thermocouple …)

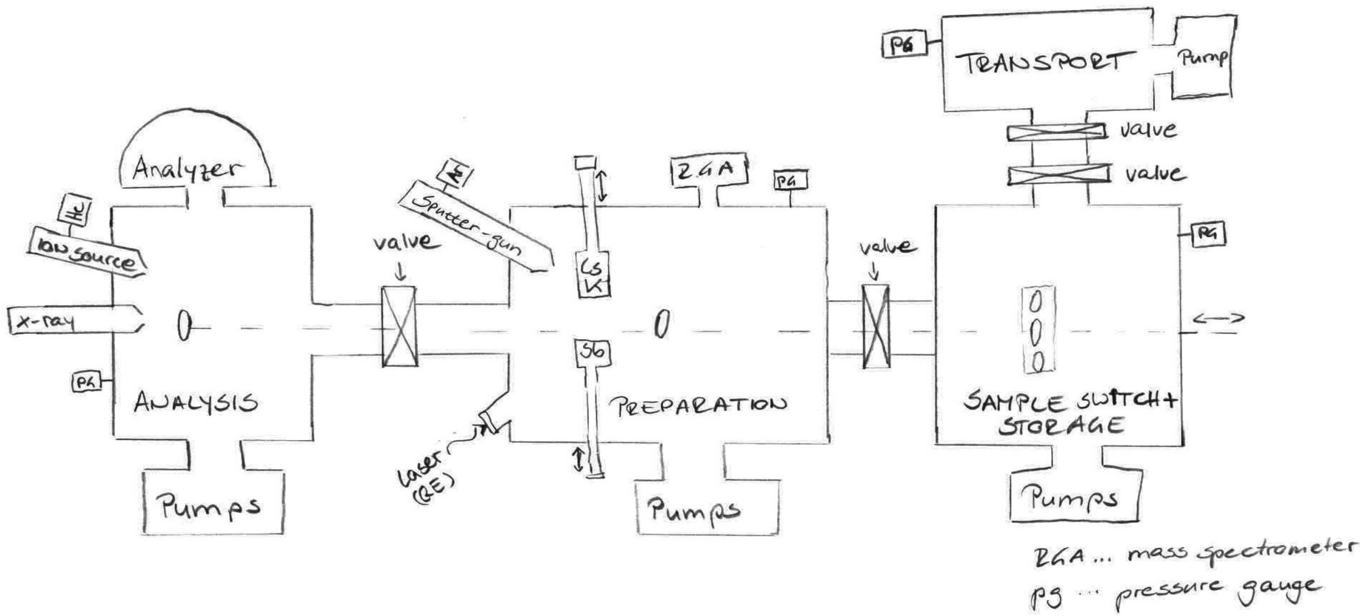

Preparation

Substrate (Mo): -polishing
-pre-treatment in UHV by ion-sputtering and heating cycles

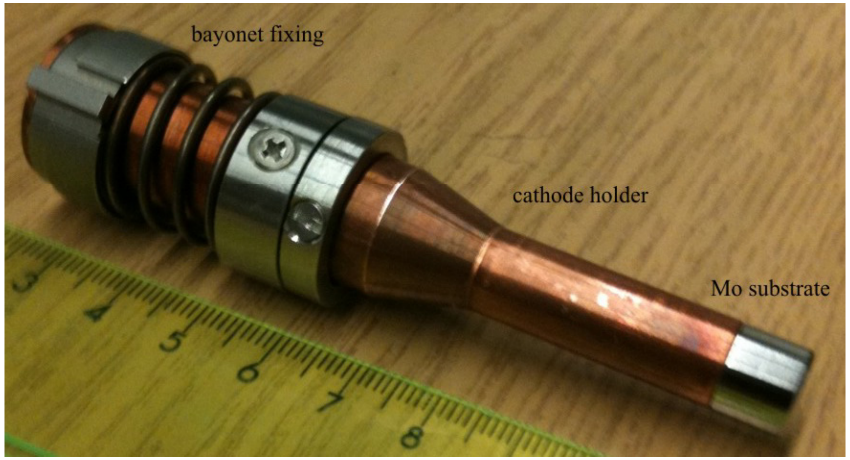

Cathode-holder from FZD

Film growth:
-elevated substrate temperature
-vapor deposition (Cs, Sb, K)

Manipulate the film appearance by:
a)substrate (element, surface roughness, pre-treatment)
b)substrate temparture
c)deposition rate and sequence
d)presence of gases (O_2, Ar)

Photoemission emittance measured in a Diode – RF Gun

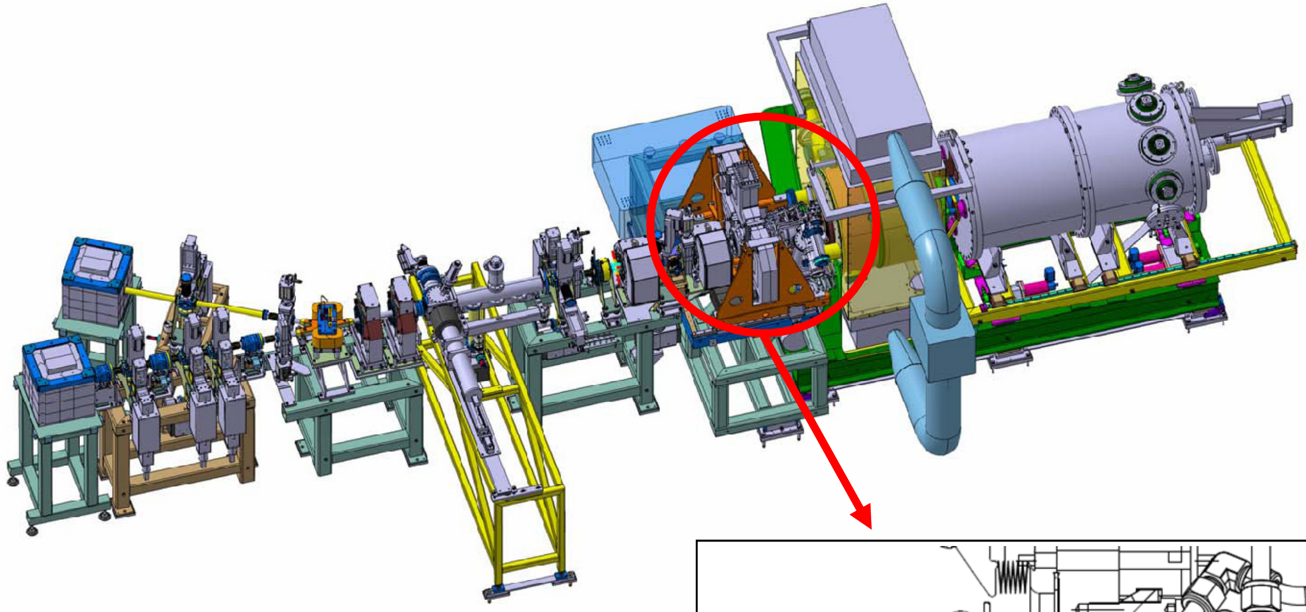

<u>Diode – RF gun Combination:</u>
Diode: 500 kV; 5 mm; < 3 Hz; Mg, Cu, …
RF: 2 Cell – L Band, 1.499 GHz
Beam: 6 MeV; 200 pC

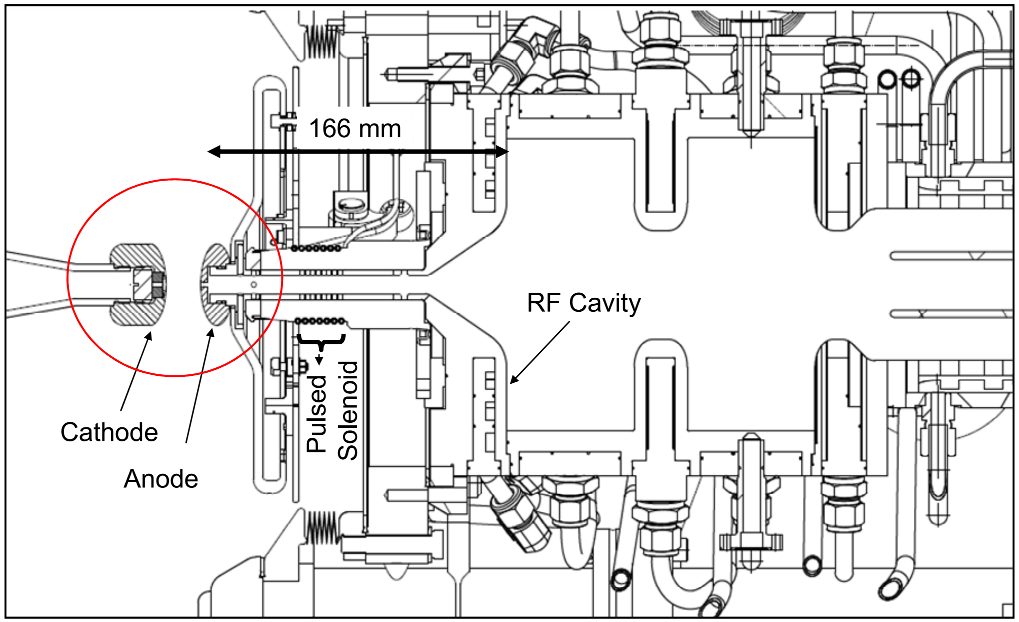

Intrinsic Emittance versus Laser Spot Size

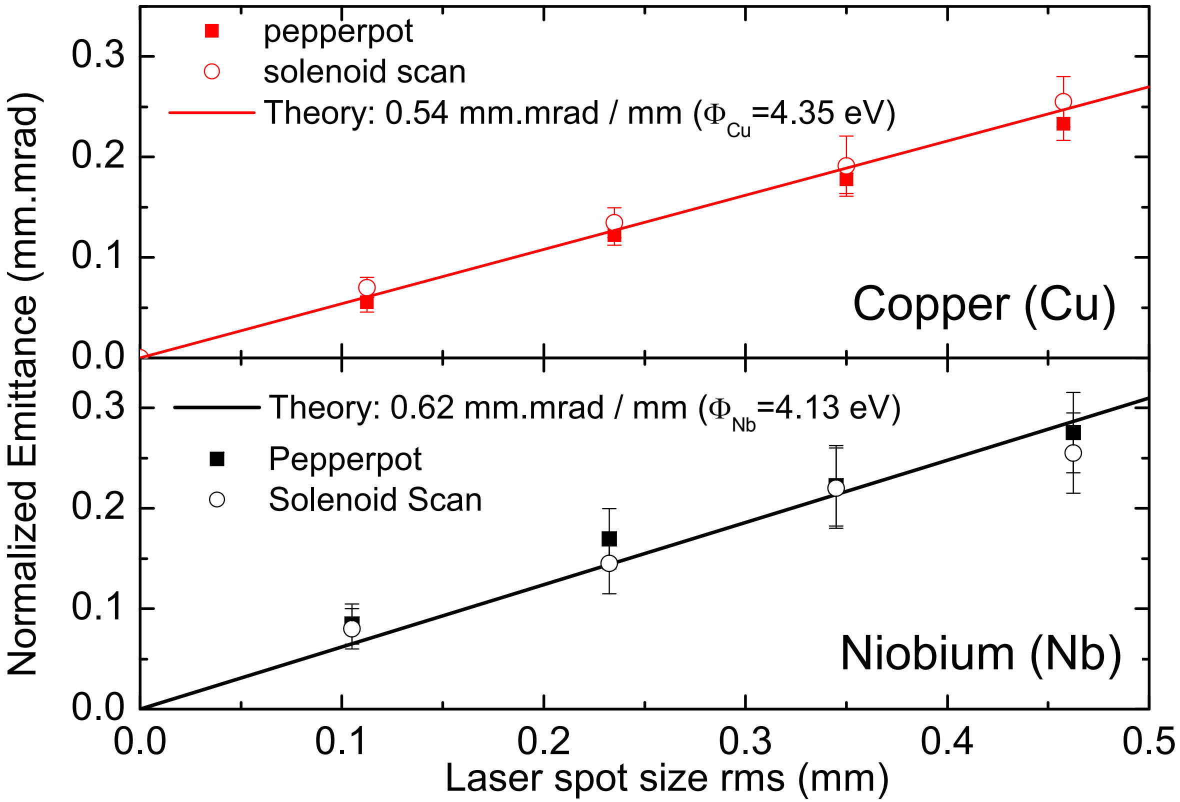

Q < 1 pC; 5.2 MeV
272 nm

$$\varepsilon_{Intrinsic} = \sigma_x \sqrt{\frac{h\nu - \Phi_0 + e^{3/2}\frac{F_{eff}^{1/2}}{(4\pi\varepsilon_0)^{1/2}}}{3mc^2}}$$

Laser spot size (rms)

Good Agreement between Pepperpot and Solenoid Scan.

Good Agreement with Theory (Linear Behavior)

Intrinsic Emittance versus Laser Wavelength

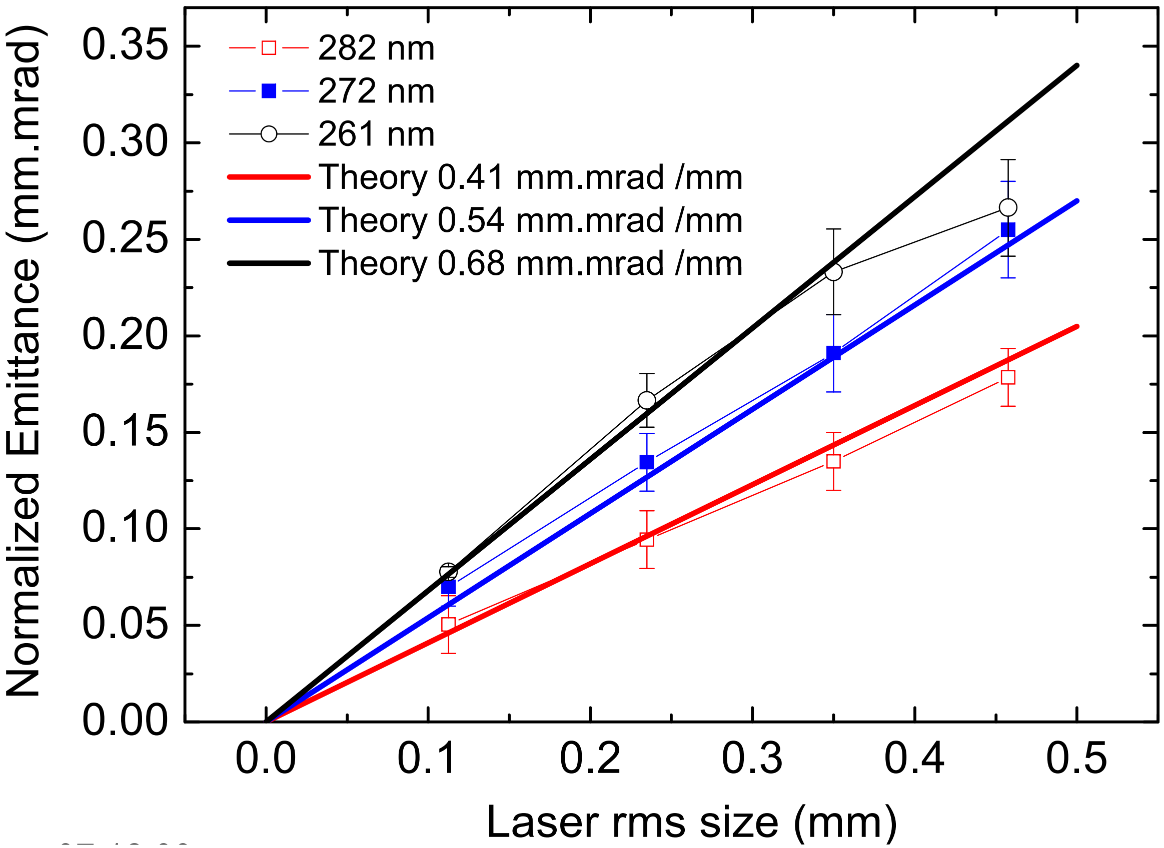

261 nm: 0.68 mm.mrad / mm

272 nm: 0.54 mm.mrad / mm

282 nm: 0.41 mm.mrad / mm

⇩

$$\varepsilon_{Intrinsic} = \sigma_x \sqrt{\frac{h\nu - \Phi_0 + e^{3/2}\dfrac{F_{eff}^{1/2}}{(4\pi\varepsilon_0)^{1/2}}}{3mc^2}}$$

⇩

Φ_{Cu}= 4.3 eV

With F_{eff} = 25 MV/m

Exp. Cond.:
Q < 1 pC; 5.2 MeV
$\sigma_{t,laser}$= 4 ps rms; 25 MV/m
Copper Cu
Solenoid Scan

PAUL SCHERRER INSTITUT

Intrinsic Emittance versus Laser Wavelength

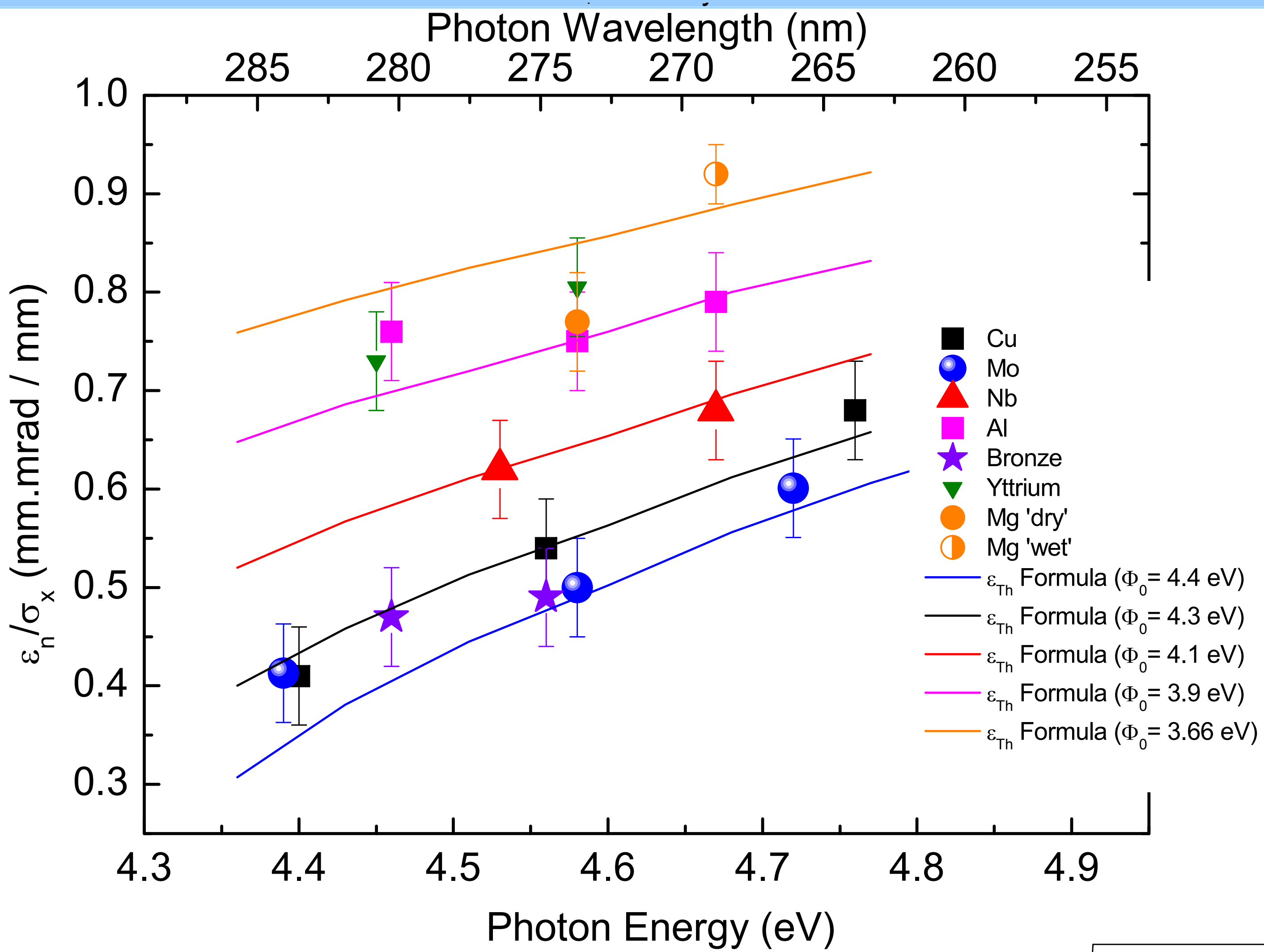

Q < 1 pC; 5 MeV; $F_{cathode}$= 25 MV/m

$$\varepsilon_{Intrinsic} = \sigma_x \sqrt{\frac{h\nu - \Phi_0 + e^{3/2}\frac{F_{eff}^{1/2}}{(4\pi\varepsilon_0)^{1/2}}}{3mc^2}}$$

Quantum Efficiency of different materials

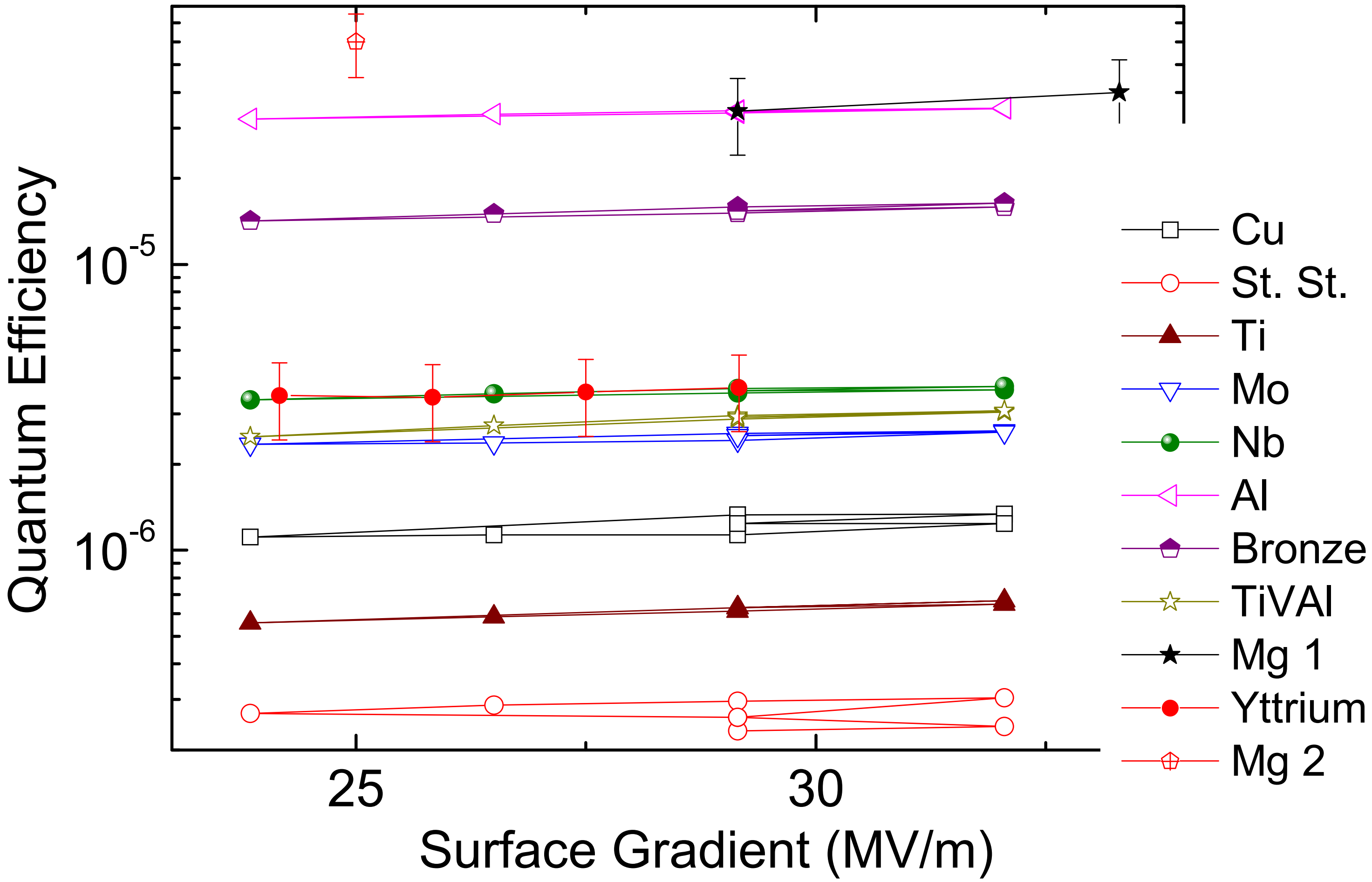

Duettino ;6 ps rms; 4-6 muJ on Cathode; 5.2 MeV; gap 6mm
DLC Hollow Cathode + Flat Insert;

Evidence of Ion Back Bombardment

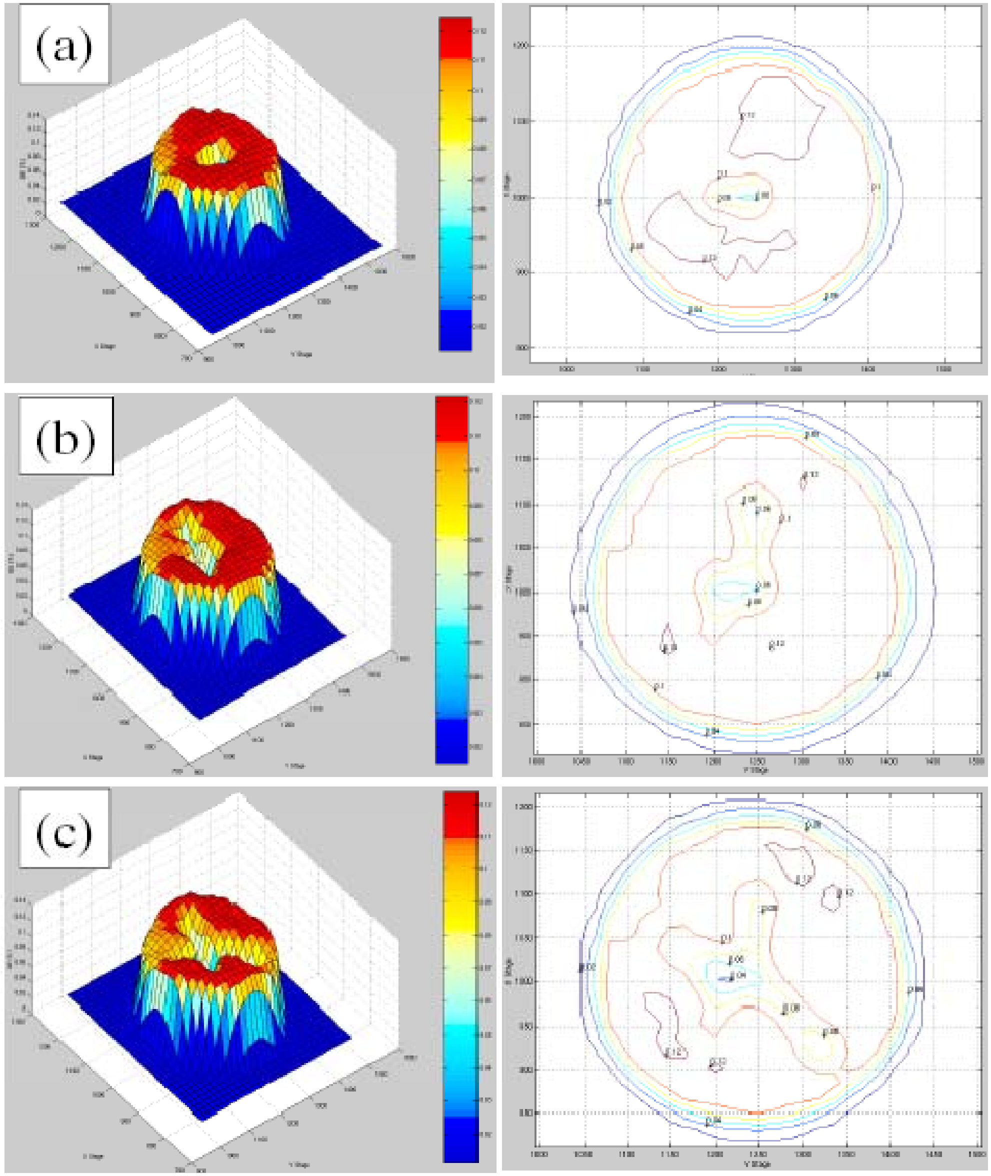

The figures show the QE degradation resulting from illumination of three separate spots over a period of many weeks. The damage appears only along a line joining the illuminated spot and the electrostatic center of the gun.

The damage is characterized (imperfectly) in terms of the Coulombs/cm^2 delivered from the illuminated spot.

C. Sinclair (Cornell)

Jlab results up to 10 mA in 100 kV Gun

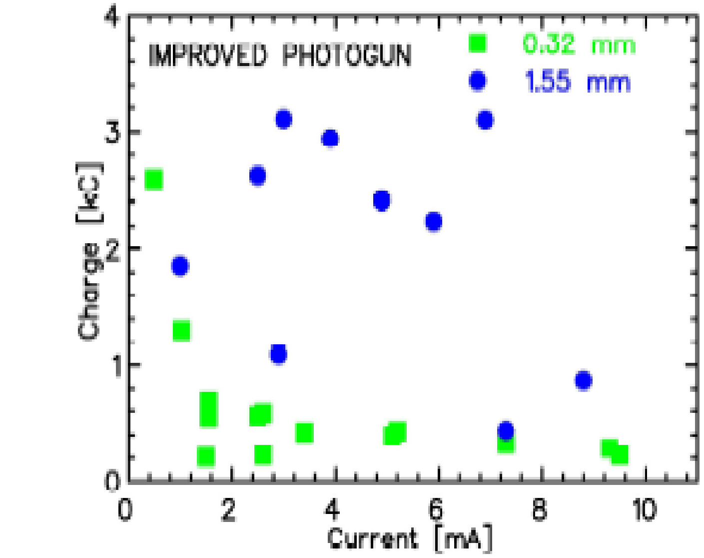

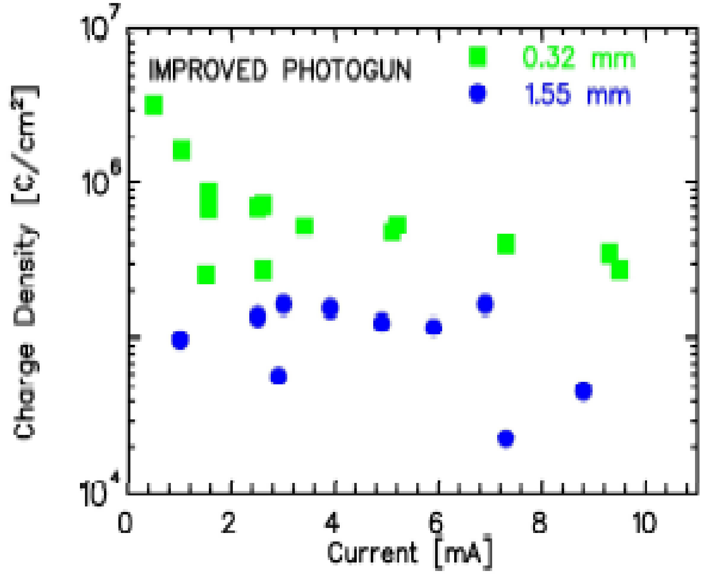

Must eliminate large radius electrons to achieve these results

Clearly factors other than the charge delivered per unit area are involved. Whether these are fundamental or not isn't clear.

From Grames et al., in *Proceedings of the 17th International Spin Symposium*, Kyoto, Japan, 2006

C. Sinclair (Cornell)

Constant Current QE Lifetime

$$T = \frac{Q_0 A}{I_0} \ln\left(\frac{P_{max} \lambda \eta_0}{1.24 I_0} \right)$$

Where Q_o is the charge density lifetime, A is the illuminated area, λ is the wavelength in μ, and P is the laser power in W.

For a Q_o of 10^6 C/cm^2 you can deliver 100 mA for 100 hours with 10 W of laser power at 527 nm on a 10% initial QE cathode, from a 1.8 mm diameter spot.

C. Sinclair (Cornell)

Complete Energy Distribution at 90K

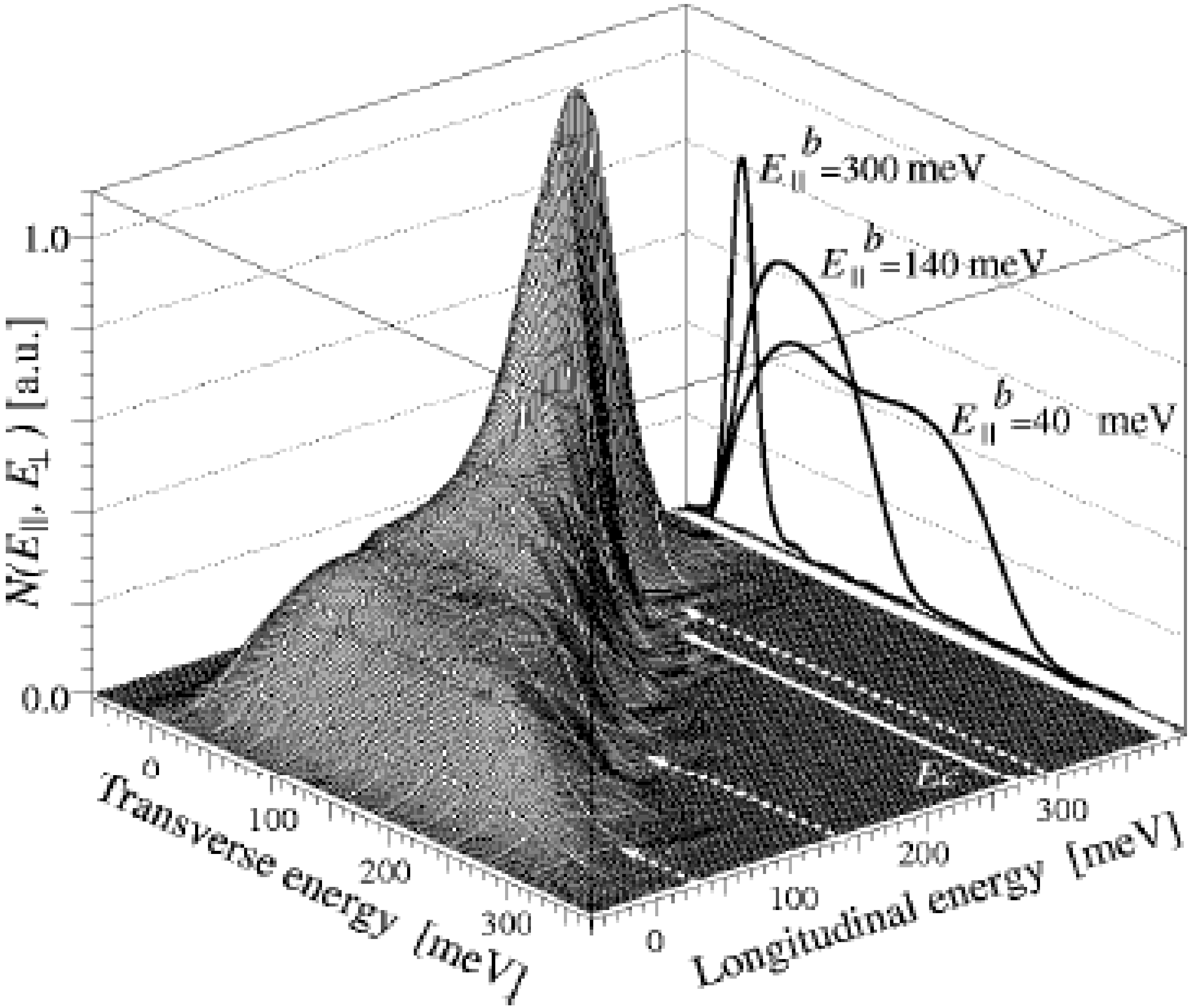

From
Orlov et al.
APL 78,
2721 (2001)

 C. Sinclair (Cornell)

Angular Distribution Measurement

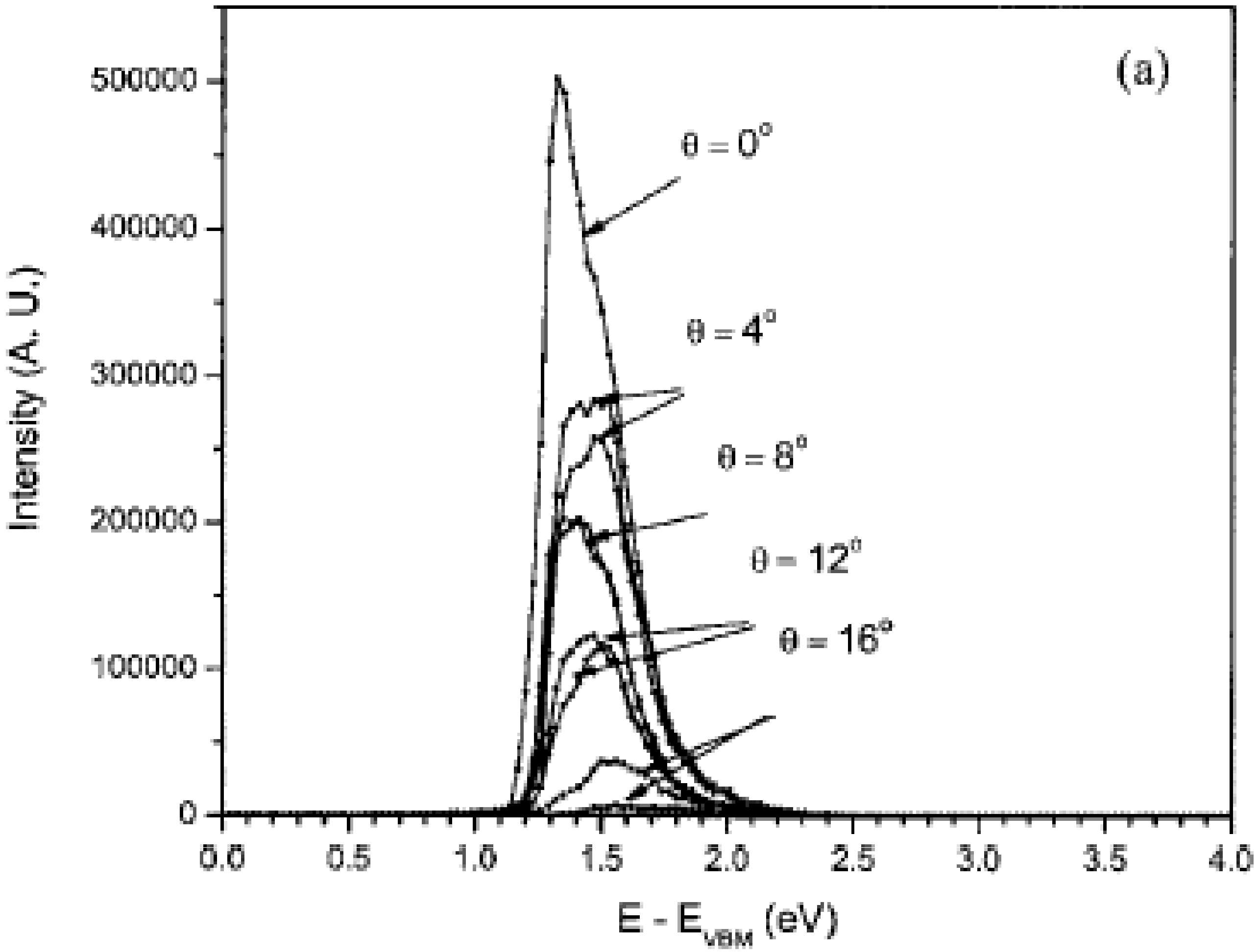

From Liu et al., JVST B 23, 2758 (2005)

Compact ERL (test facility)

M.Yamamoto (KEK)

Parameters of the Compact ERL

	Parameters
Beam energy	35 - 245 MeV
Injection energy	5 MeV
Average current	10 - 100 mA
Acc. gradient (main linac)	15 MV/m
Normalized emittance	0.1 - 1 mm·mrad
Bunch length (rms)	1 - 3 ps (usual) ~ 100 fs (with B.C.)
RF frequency	1.3 GHz

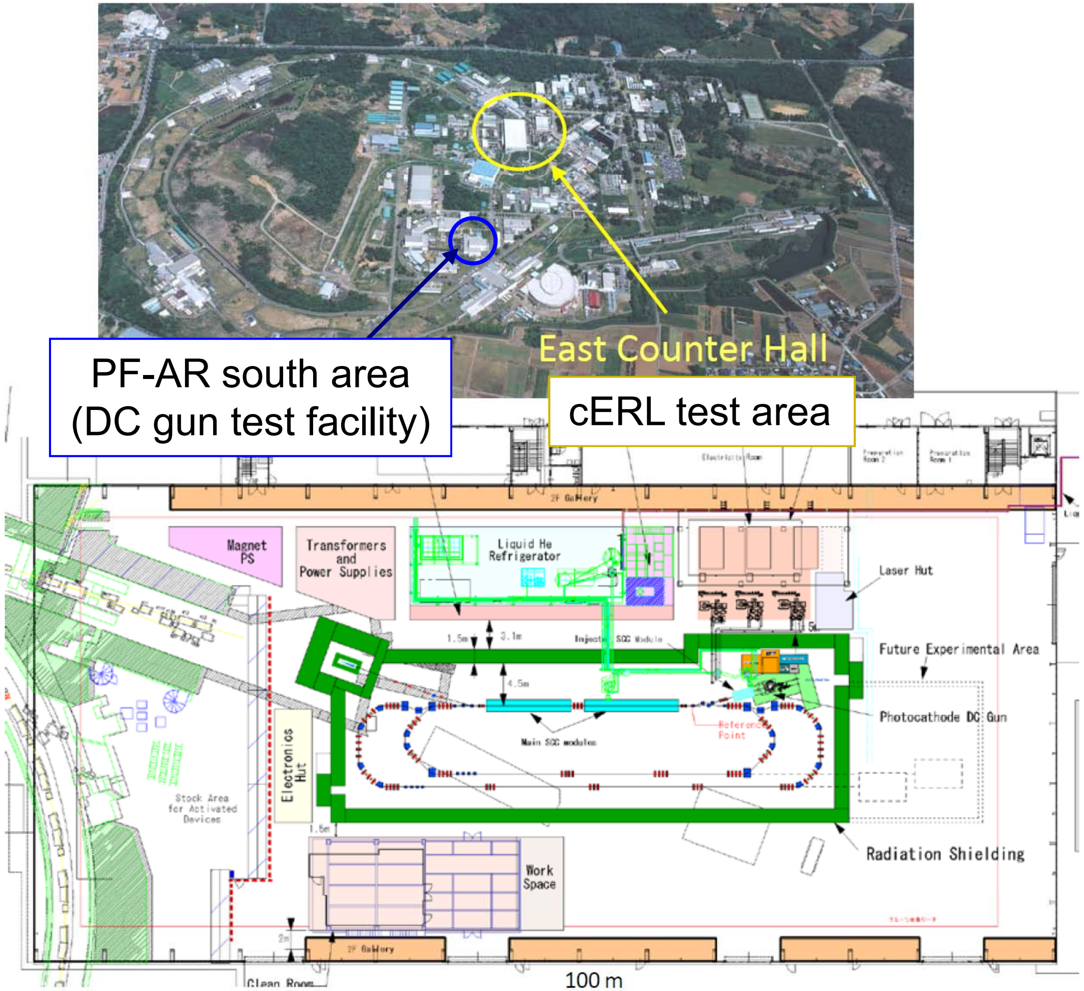

Commissioning will be started end of 2012 FY.

Policy of cathode R&D for ERL

M.Yamamoto (KEK)

- Superlattice structure for ultra low emittance
  - narrow conduction mini-band width
  - higher conduction mini-band level
- High QE cathode for reducing laser power
  - DBR structure
  - control density of state (SL)
  - wide band gap material
- Transmission type cathode for suppression laser heating
  - transmitting substrate
  - high thermal conductivity substrate

Laser system for injector commissioning at KEK

M.Yamamoto (KEK)

- Drive laser for AR-south injector commisioning test area (started since 2009)
- Requirement for 10mA operation of cERL: 1.3GHz(repetition), 530nm(wavelength), 20ps(pulse duration), 1.5W(power)
- System has been built based on commercial units (1.3GHz oscillator, fiber amplifier, SHG, etc.)
- 500mW (2ω) output has been achieved. Enough for first commisioning of the injector upto 3mA. Development of higher power amplifier is on going.

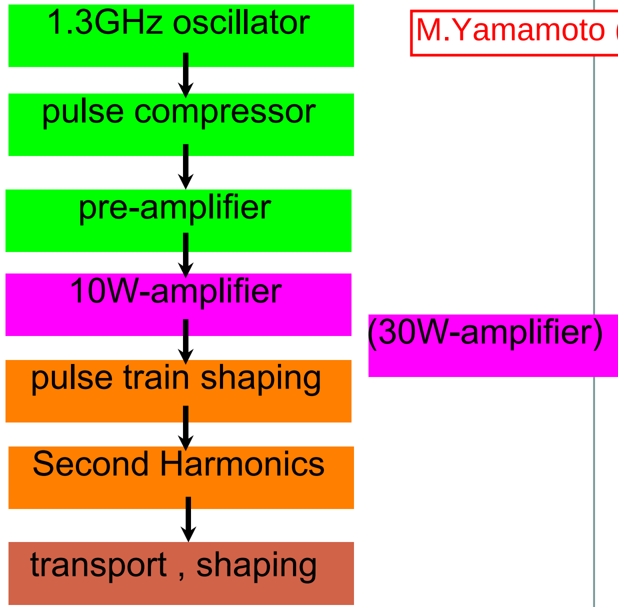

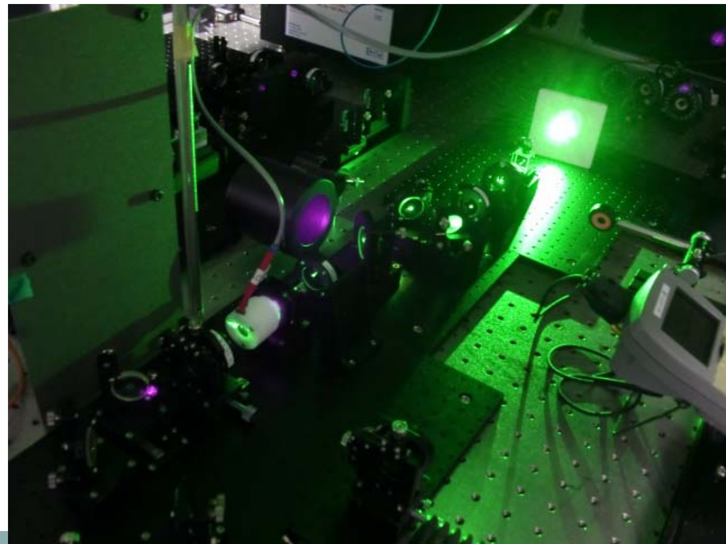

200 kV DC Gun

M.Yamamoto (KEK)

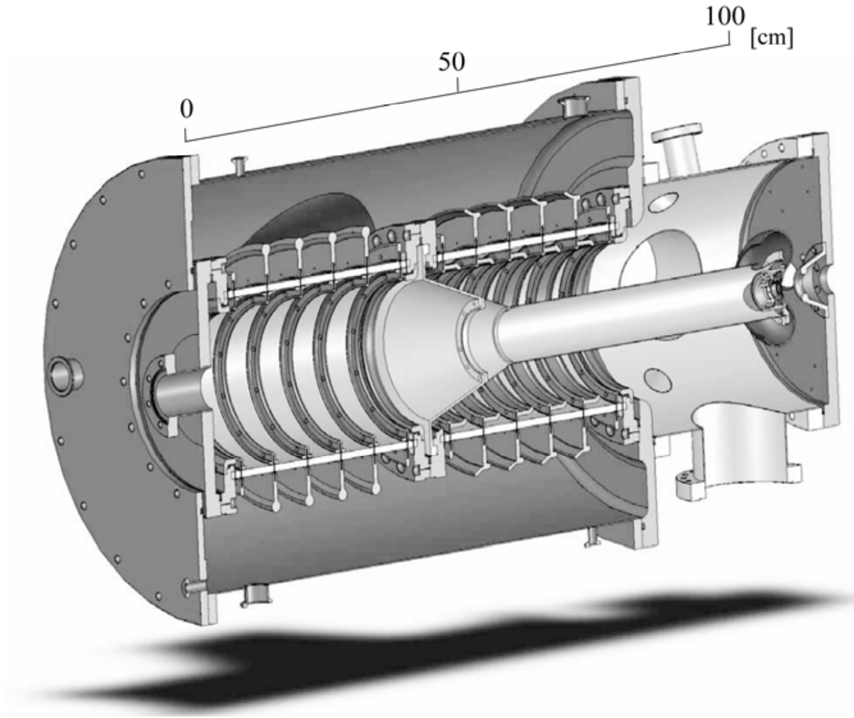

Ti anode & Mo cathode, E_{cath}: 3.0 MV/m
Segmented insulators, Ultimate P: 2E-9 Pa

200 kV polarized electron gun (NPES3) has been developed at Nagoya Univ. Details was presented in PESP2008.

The gun was transferred from Nagoya to KEK in 2009.

Layout of Beam Diagnostic Line

M.Yamamoto (KEK)

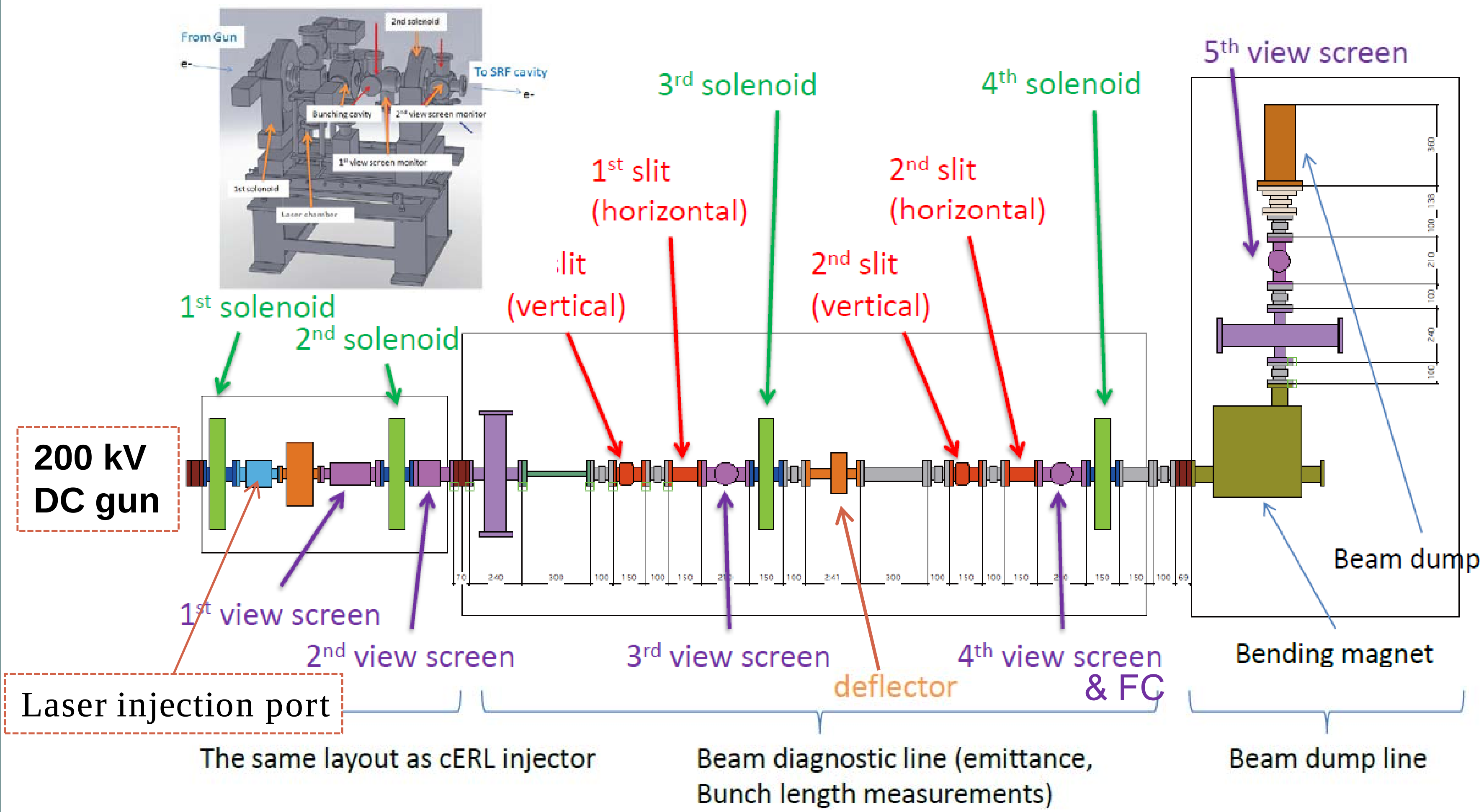

Emittance measurement result (SL)

M. Kuwahara (Nagoya)

- Photon energy dependence (SL and Bulk-GaAs)

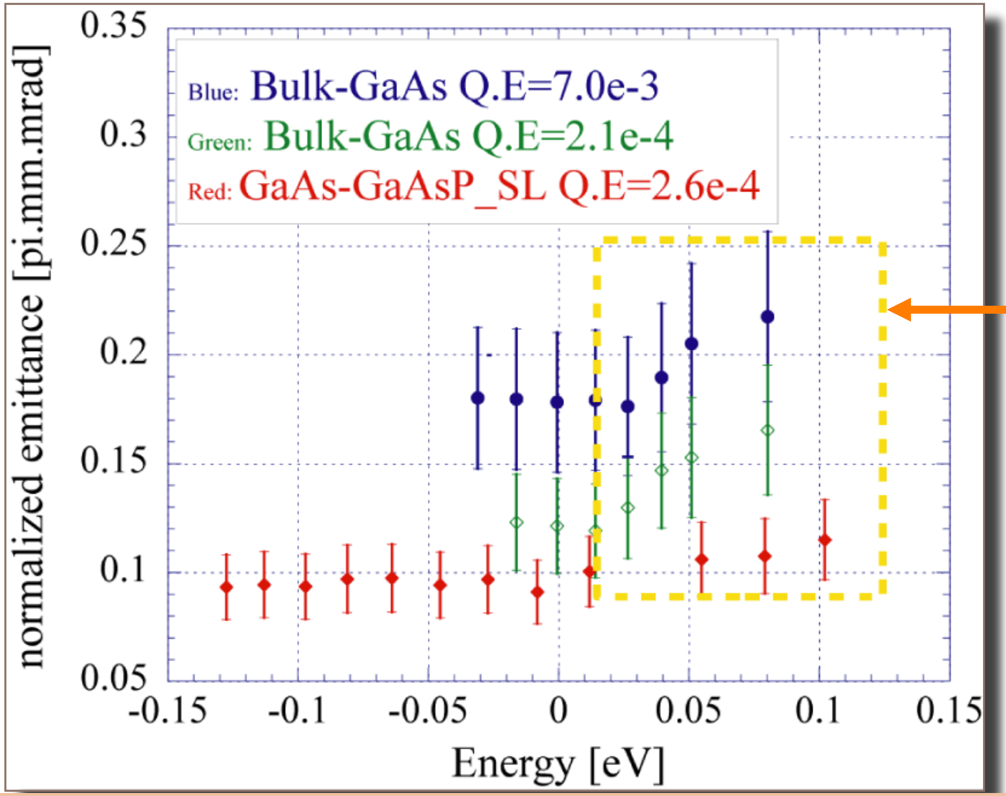

In SL photocathode, the increase of emittance is lower than that of bulk-GaAs

This effect is explained by the dispersion of the JDOS.

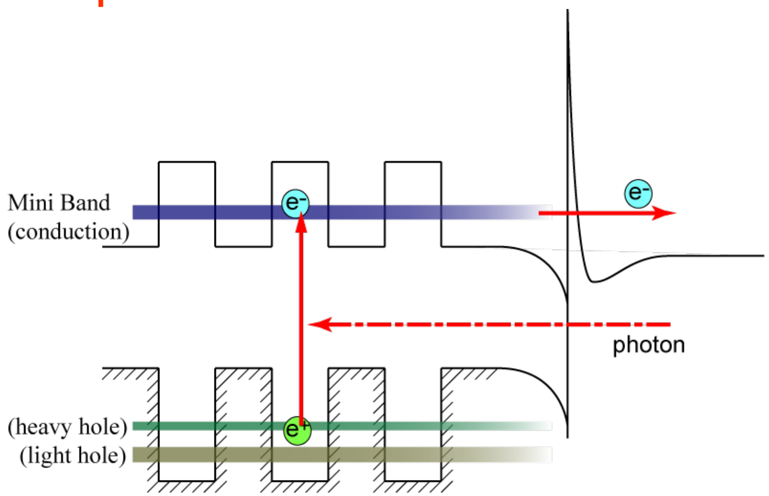

The DOS in C.B. is quantized and shrinks.
(Miniband is formed by the micro-structure.)

⇒ An emittance growth is suppressed in shorter wavelength
SL structure has a low emittance with high QE comparing with a bulk-GaAs

Superlattice photocathode

M. Kuwahara (Nagoya)

Toward a low emittance with a high QE

1. Layer-structure -> SL (suppressing the emittane growth with increasing the excitation energy)
2. Using excitation both of HH and LH
3. Expand the active layer with suppressing the expansion of pulse width

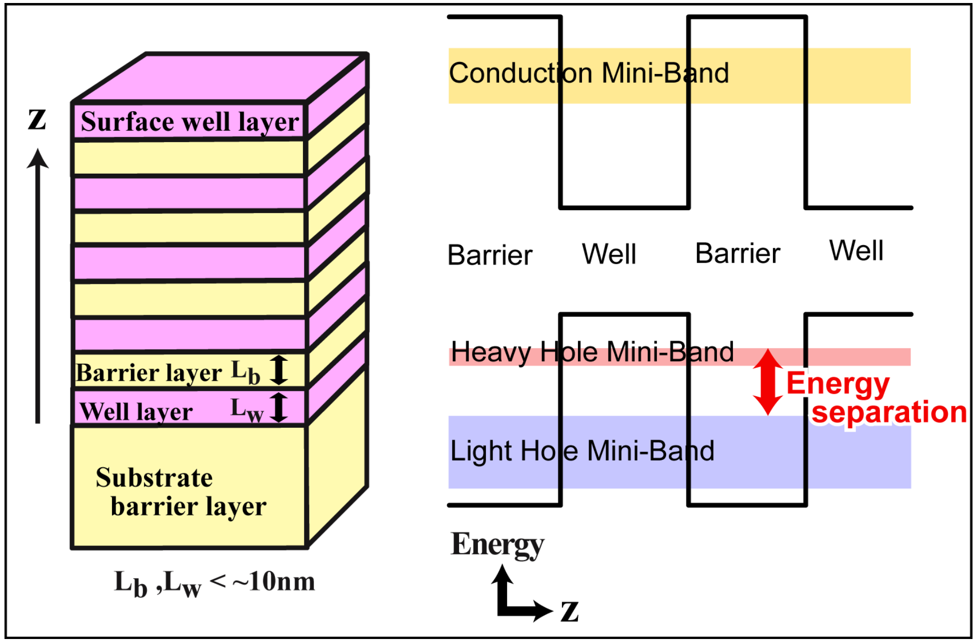

The JDOS of C.B. is quantized and shrinks.
(Miniband is formed by the superlattice)

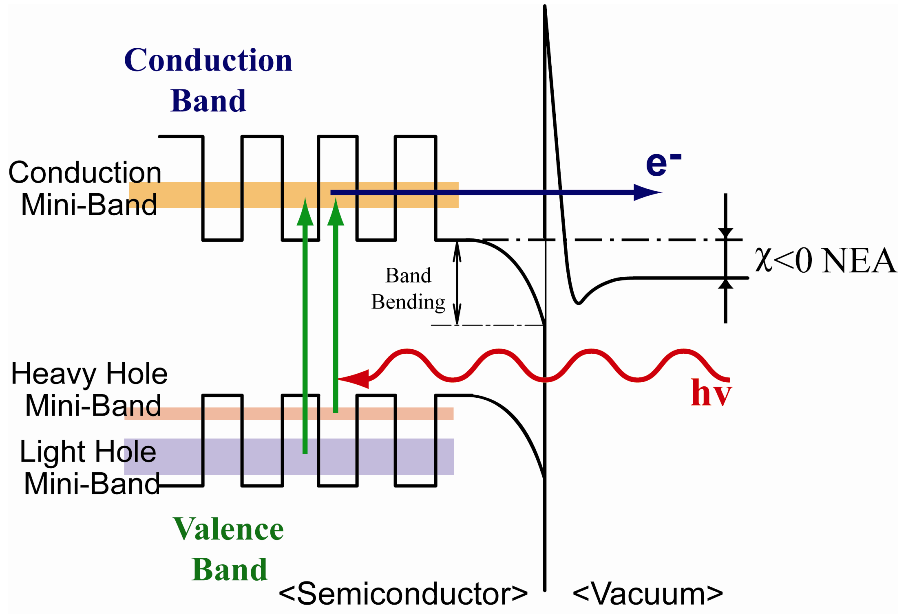

Schematic of an extraction process in a SL photocathode

Superlattice photocathode

M. Kuwahara (Nagoya)

- Excitation energy toward the high QE
  - Joint Density of State

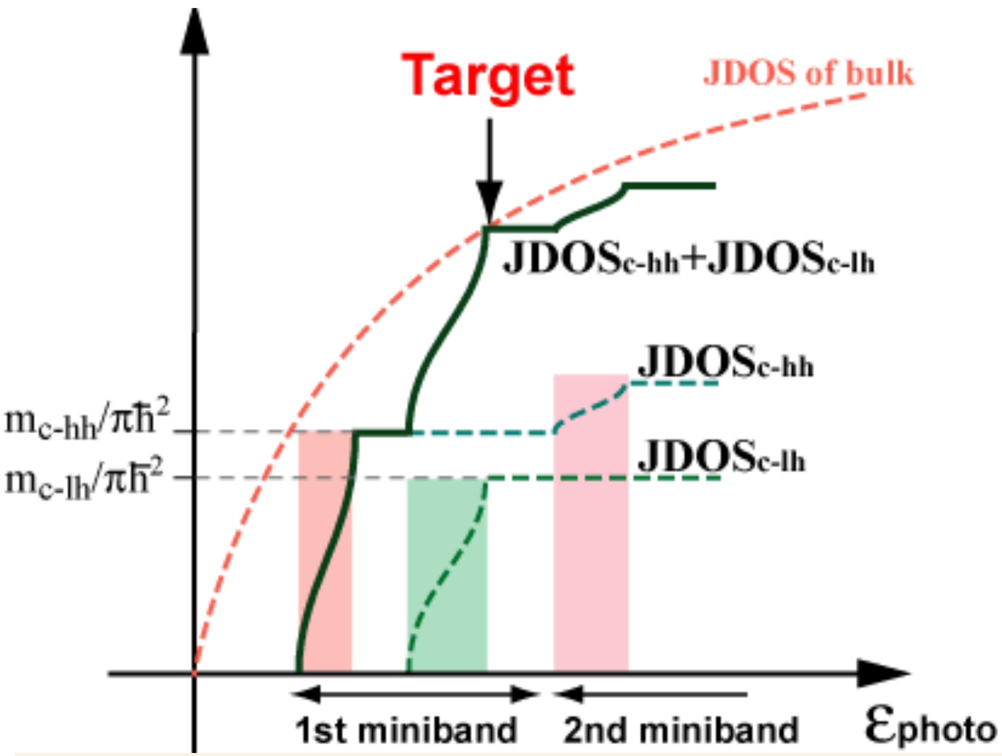

The Brillouin zone depends the SL repetition

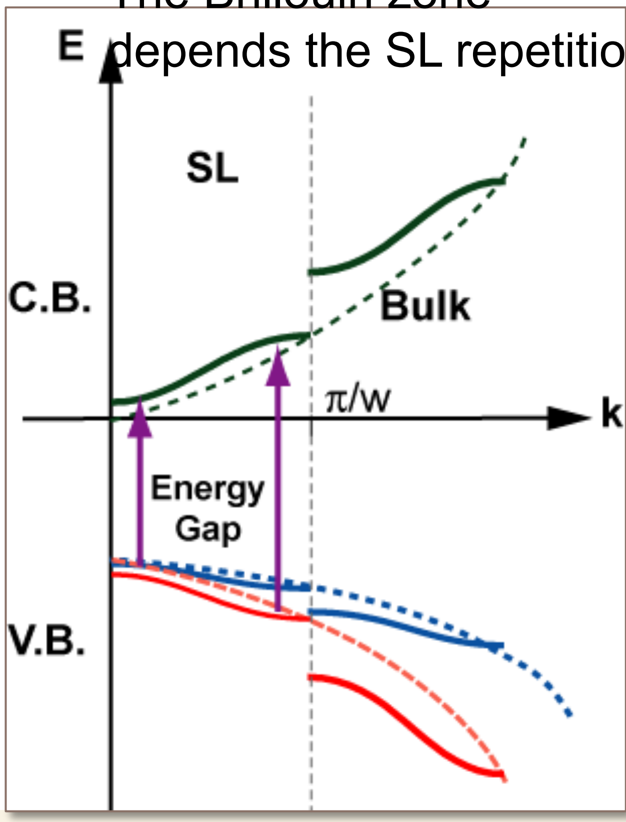

The dispersion of JDOS is dominantly determined by the C.B. because the effective mass is smaller than that of V.B.
Separation between 1st and 2nd mini-band in C.B. must be larger than that of HH and LH.

Temporal response in SL (not in Bulk)

M. Kuwahara (Nagoya)

- Average emission time

In Bulk-GaAs, the pulse width is mainly determined by the absorption length. However, if the active-layer thickness is limited, the tail can be cut.

$$\langle t \rangle \approx \frac{d^2}{12D} = \frac{d^2}{12 \cdot 27cm^2/s} = 2ps$$

$$d \sim 254nm$$

$GaAs/GaAsP \;\; Supperlattice$

$\tau_{re} = 55ps, \tau_s = 140ps, \alpha = 7 \times 10^3 cm^{-1}$

$D = \mu_e k_B T/e = 1000cm^2/Vs \cdot 27mV = 27cm^2/s$

Ref.: K. Aulenbacher, et al., J. Appl. Phys. 92 (2002) 7536.

Using the QE of 0.9% @751nm in active-layer width of 96nm,

In the case of 254-nm width, QE is expect to be 2.1%. (Without recombination effect)

- Simple estimation using Pol. , relaxation time and recombination time

$$P_{CW} = P_0 \frac{\alpha\langle v\rangle + 1/\tau_r}{\alpha\langle v\rangle + 1/\tau_s + 1/\tau_r} \frac{1 - \exp\left(-(\alpha\langle v\rangle + 1/\tau_s + 1/\tau_r) \cdot d/\langle v\rangle\right)}{1 - \exp\left(-(\alpha\langle v\rangle + 1/\tau_r) \cdot d/\langle v\rangle\right)} = 0.92$$

$\langle v\rangle \approx 9 \times 10^4 m/s$

$\langle t\rangle = 96nm/\langle v\rangle \approx 1ps$

Corresponding with the temporal response time in short pulse

The difference ~ additional spin-relaxation time or scattering in drifting process or BBR ?

Recent R&D

M. Kuwahara (Nagoya)

A transmission-type spin-polarized photocathode has been developed for application to several types of electron microscopy, e.g., spin-polarized LEEM, spin-polarized TEM and so on.

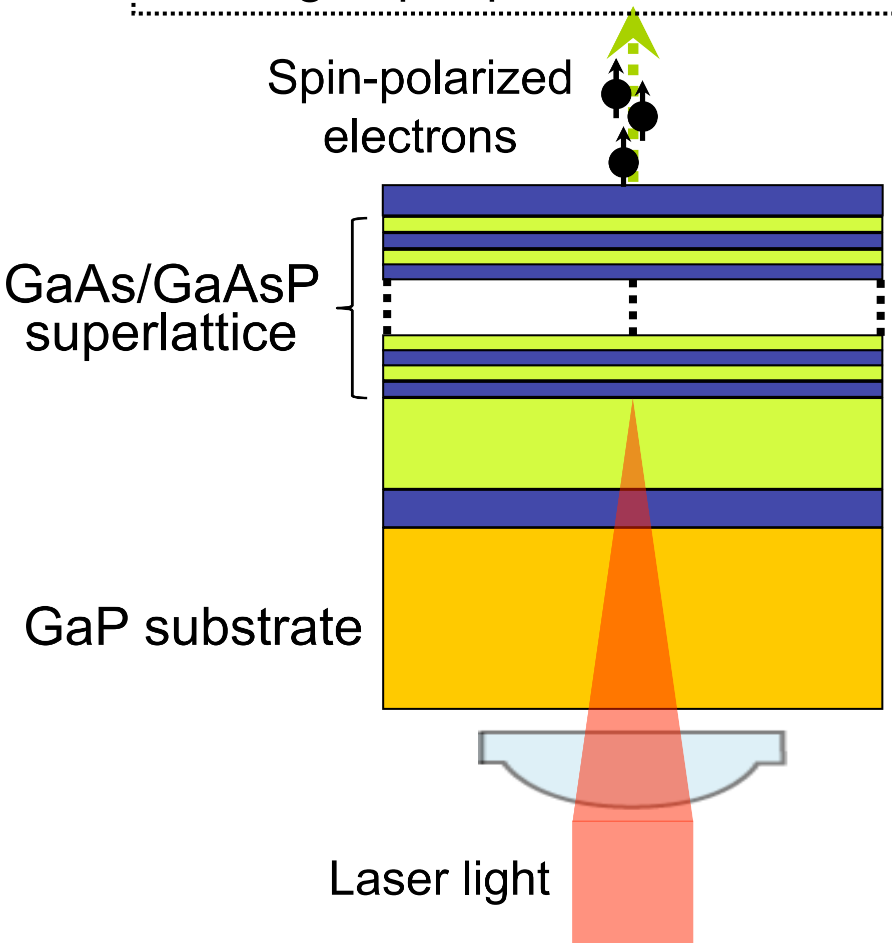

Transmission-type photocathode with GaAs/GaAsP strained superlattice

- High spin-polarization : **90%**
- Super-high brightness : **1.3×10^7 A·cm^{-2}·sr^{-1}** (@20 kV)

Xiuguang JIN et al., Appl. Phys. Express **1** (2008) #045002

まとめ

・現状のカソード材料について、様々な手法で表面分析が進められている。（BNLではNSLSを利用した表面・構造分析が実際に行われている。（見学コース））

・アメリカ各所では、カソード開発・分析（特にその場観測）を各所で協力して行う体制を模索している。
（カソードPuck、真空スーツケースの規格化）

・カソード開発のためのシミュレーションコードの開発が進んでいる。

・マルチアルカリカソード、酸化膜カソードなどの使用を検討している所が多い。（高QE, カソード寿命の点で。）

・カソードとペアで考えるべきレーザーに関する議論はほとんど無かった。
・2年後にコーネル大で2回目を開催予定。